

CHALMERS



Erosion of Silica Sol in Post Grouted Tunnel at Great Depth

*Master of Science Thesis in the Master's Programme Infrastructure and
Environmental Engineering*

REYNIR ÖRN REYNISSON

Department of Civil and Environmental Engineering
Division of GeoEngineering
CHALMERS UNIVERSITY OF TECHNOLOGY
Göteborg, Sweden 2014
Master's Thesis 2014:105

MASTER'S THESIS 2014:

Erosion of Silica Sol in Post Grouted Tunnel at Great Depth

*Master of Science Thesis in the Master's Programme Infrastructure and
Environmental Engineering*

REYNIR ÖRN REYNISSON

Department of Civil and Environmental Engineering

Division of GeoEngineering

CHALMERS UNIVERSITY OF TECHNOLOGY

Göteborg, Sweden 2014

Erosion of Silica Sol in Post Grouted Tunnel at Great Depth
*Master of Science Thesis in the Master's Programme Infrastructure and
Environmental Engineering*
REYNIR ÖRN REYNISSON

© REYNIR ÖRN REYNISSON), 2014

Examensarbete / Institutionen för bygg- och miljöteknik,
Chalmers tekniska högskola 2014:

Department of Civil and Environmental Engineering
Division of GeoEngineering
Chalmers University of Technology
SE-412 96 Göteborg
Sweden
Telephone: + 46 (0)31-772 1000

Reproservice, Chalmers University of Technology
Göteborg, Sweden 2014

Erosion of Silica Sol in Post Grouted Tunnel at Great Depth
*Master of Science Thesis in the Master's Programme Infrastructure and
Environmental Engineering*
REYNIR ÖRN REYNISSON
Department of Civil and Environmental Engineering
Division of GeoEngineering
Chalmers University of Technology

ABSTRACT

Due to planned construct of a repository for nuclear waste in crystalline rock at great depth, the Swedish Nuclear Fuel and Waste Management Co (SKB) have built the testing facility Äspö HRL to develop and test geotechnical methods and to obtain a safe and fully functional repository at such a great depth. To examine the performance of grouting and to test different drilling techniques and explosive and borehole layouts at great depth, a small tunnel called TASS, located in the Äspö HRL facility, was excavated at a depth of 450 m. Requirements of inflow after pre-grouting were not fulfilled over stretch 34-50 m, the stretch was therefore post-grouted to fulfill the requirement. Since the stretch was post-grouted inflow into the tunnel stretch has increased and is still rising. The main aim of this project is to develop a hypothesis about why leaking boreholes occur even though it is sealed. The report is based on a literature study, borehole data and visual inspection in the TASS tunnel. The development of the hypothesis will be based on analysis of inflow data, geological condition, hydrogeology, properties of the grouting material and the grouting procedure.

The study has shown that the cause of leaking post-grouted boreholes is difficult to explain. This study has shown that a very high hydraulic gradient can be expected in the pre-grouted zone as well a high gradient outside the pre-grouted zone. The post-grouting mostly took place in un-grouted rock which is likely to contain relatively large apertures. With a high hydraulic gradient and large apertures a high shear stress caused by groundwater can be expected thus increasing the risk of erosion. Other factors that are likely to affect the shear strength of the silica sol are the temperature inside the rock and the dilution of the grouting material during grouting. It is likely that the early shear strength of the silica sol was never sufficient to withstand the groundwater shear stress.

Key words: post-grouting, sealing, penetration length, overlap, silica sol, hydraulic gradient, apertures, groundwater shear stress, shear strength of silica sol, temperature, dilution

Contents

1	INTRODUCTION	1
1.1	Aim and objectives	2
1.1.1	Objectives of this thesis	2
1.2	Limitations	2
1.3	Background	3
1.3.1	Description of Äspö and TASS tunnel	3
1.3.2	Local geology	4
1.3.3	Geological mapping of the TASS tunnel	5
1.3.4	Description of grouting layout	8
1.4	Methodology	9
2	THEORY	11
2.1	Geological mapping	11
2.2	Description of fractures in hard rock	12
2.3	Hydrogeology of bedrock	13
2.3.1	Fracture flow	13
2.3.2	Flow dimensions	15
2.3.3	Transmissivity distributions	16
2.3.4	Hydraulic gradient and inflow to a tunnel	17
2.4	Grouting	20
2.4.1	Silica Sol	22
2.4.2	Rheology and strength of Silica Sol	23
2.4.3	Penetrability and penetration length	26
2.4.4	Grouting pressure and flow	28
2.5	Erosion	28
3	RESULTS	31
3.1	Rock mass and fractures interpretation	31
3.2	Inflow and pressure analyses	31
3.3	Fractures transmissivity and apertures	32
3.4	Penetration length based on natural inflow	33
3.5	Hydraulic gradient	35
3.5.1	Theoretical gradient	35
3.5.2	Simplified and “worst case” gradient	36
3.5.3	Gradient according to geometry	37
3.6	Shear stress of water – Erosion	37
3.7	Field trip to TASS	38
4	DISCUSSION	40

5	CONCLUSION AND FURTHER WORK	44
6	REFERENCES	44

Preface

The work presented in this thesis was carried out at the Department of Civil and Environmental Engineering, Division of GeoEngineering at Chalmers University of Technology, Sweden. The work of this master thesis has been carried out from January 2014 to June 2014. It has been supervised by Johan Funehag (Chalmers University of Technology) and is he also the examiner of the project.

I wish to express my gratitude to all whom have contributed to the progress of this master thesis project. First of all I would like to thank my supervisor for his support and guidance during the progress of this thesis. Many thanks also to Ann Emmelin for the guidance through the Äspö HRL facility and Patrick O'Malley for his comments. Special thanks to my opponent, Linn Ödlund Eriksson for useful comments throughout the project.

Finally, I would like to thank my family, friends and my girlfriend for their support, patience and understanding.

Göteborg, June 2014

Reynir Örn Reynisson

Notations

Roman upper case letters

A	[m ²]	Area
H	[m]	Groundwater head
I_D	[-]	Relevant penetration
I_{1-D}	[m]	Penetration length for 1-D flow
$I_{max,2-D}$	[m]	Penetration length for 2-D flow
K	[m/s]	Hydraulic conductivity
L	[m]	Length of tunnel section
T	[m ² /s]	Transmissivity
T_0	[m ² /s]	Transmissivity of undisturbed rock
T_{inj}	[m ² /s]	Transmissivity of grouted zone
$P_{borehole}$	[Pa]	Acting pressure in borehole
Q	[m ³ /s]	Flow
Q_T	[m ³ /s]	Inflow into the tunnel per length

Roman lower case letters

a		
b_{hyd}	[m]	Hydraulic aperture
c		Contact area between fracture planes
g	[m/s ²]	Acceleration due to gravity
h	[m]	Height
p_w	[Pa]	Groundwater pressure
q_f	[m ² /s]	Flow in fracture
r	[m]	radius of tunnel and sealed zone
r_b	[m]	Borehole radius
r_t	[m]	Tunnel radius
t	[m]	Thickness of grouted zone
t_G	[s, min]	Gel induction time
v_f	[m/s]	Mean velocity in slot
w	[m]	Width
x	[m]	Grouted distance
z	[m]	Depth

Greek upper case letters

Δp		Pressure difference
------------	--	---------------------

Greek lower case letters

$\dot{\gamma}$	[s ⁻¹]	Shear rate
θ	[-]	Parameter for penetration analysis
μ	[Pas]	Viscosity
μ_0	[Pas]	Initial viscosity
τ	[Pa]	Shear stress
τ_f	[Pa]	Shear strength
τ_0	[Pa]	yield stress
ξ	[-]	Skin factor
ρ	[kg/m ³]	Density
ρ_w	[kg/m ³]	Density of water

Mathematical expressions

$-\frac{dh}{dx}$	[-]	Hydraulic gradient
$\frac{Q}{dh}$	[m ² /s]	Specific capacity

Abbreviations

HRL	Hard Rock Laboratory
SGU	Sveriges Geologiska Undersökning Geological Survey of Sweden
SKB	Svensk Kärnbränslehantering AB Swedish Nuclear Fuel and Waste Management Co
TBM	Tunnel Boring Machine
TIB	Transscandinavium Igneous Belt
WPT	Water Pressure Test

1 Introduction

The Swedish Nuclear Fuel and Waste Management Co (SKB) has planned to construct a repository for nuclear waste in crystalline rock at a depth of 400-500 m in the coming years. To develop and test geotechnical methods and to obtain a safe and fully functional repository at such a great depth, Äspö Hard Rock Laboratory (Äspö HRL) has built as a testing facility. The knowledge gathered from Äspö HRL will then be used during the construction of the final repository.

Underground constructions are likely to face inflow problems if they are located below groundwater level. Groundwater flow mainly exists in fractures that have been formed by deformation in brittle rock through the ages. To prevent or/and maintain acceptable inflow into underground constructions such as tunnels, grouting is often carried out to seal the construction. Groundwater pressure increases with depth and can cause a high hydraulic gradient towards the tunnels.

In 2006, SKB decided to use silica sol as an alternative and/or complement to cement-based grout for sealing in the TASS Tunnel. Silica sol is a chemical compound that is environmentally friendly and therefore preferable as a grouting material. An advantage of silica sol is that it can seal very narrow fractures, approximately 0.01 mm in aperture. On the other hand, silica sol had yet to be tested deep underground and SKB therefore decided to investigate its properties at depth (Sigurdsson & Hardenby, 2010).

To examine the performance of grouting and to test different drilling techniques and explosive and borehole layouts at depth, a small tunnel called TASS, located in the Äspö HRL facility, was excavated at a depth of 450 m. TASS is located in rock with limited fracture frequency and water inflow. The total length of the Äspö HRL tunnels is 3,600 m, excavated mostly using the conventional drill and blast method. The final 400 m were excavated using a tunnel boring machine (TBM).

After pre-grouting the whole tunnel, the water inflow was 1.3 l/min per 60 m of tunnel. The inflow requirement for the TASS Tunnel was set at 1 l/min per 60 m of tunnel (Sigurdsson & Hardenby, 2010). Sections 10-34 m and 50-81 m both met the requirements. However, section 34-50 m did not and was therefore complemented with a post-grouting campaign.

Directly after post-grouting, the inflow into the tunnel section was approximately 0.6 l/min per 60 m. This inflow subsequently increased to 1.2 l/min per 60 m in 2010 and is still rising (Funehag, Unpublished). In order to find out why inflow is increasing, an analysis of the inflow data needs to be made. An examination of the geological and hydraulic properties will also be made as well as the grout properties and grouting procedure.

1.1 Aim and objectives

The main aim of this project is to develop a hypothesis about why leaking boreholes occur in the TASS Tunnel at the Äspö Hard Rock Laboratory (HRL) even though it is sealed. The hypothesis will be based on information from the literature study, borehole data and visual inspection in the TASS tunnel.

1.1.1 Objectives of this thesis

The report is based on a literature study that compiled theory and knowledge about the objectives. The following will be considered for the development of the hypothesis:

- Analysis of inflow data from post-grouting boreholes.
- Local geology and geological condition of bedrock will be inspected.
- Analysis of the hydrogeology of leaking boreholes, such as transmissivity, aperture of fractures and the hydraulic gradient.
- The properties of the grout, gel time and shear strength will be inspected.
- The grouting procedure, such as injection time and pressure.

1.2 Limitations

This project will only examine section 34-50 m in the TASS Tunnel and will evaluate data from post-grouted boreholes. A theoretical approach will be the main focus in the project and all information and data are obtained from the Äspö HRL. At the end of the project, the Äspö Hard Rock Laboratory will be visited to validate the results.

1.3 Background

The following chapter will include a description of the Äspö HRL facility and the TASS Tunnel as well as the local geology, the hydrogeology and the grouting layout in the TASS Tunnel.

1.3.1 Description of Äspö and TASS tunnel

Äspö HRL is located in the Simpevarp area in the municipality of Oskarshamn, which is on the south-east coast of Sweden. The facility is an important part of SKB's work on the design and construction of a repository for the final disposal of spent nuclear fuel and was brought into operation in 1995. The main reason for building Äspö HRL is to give scientists the opportunity to research and demonstrate methods suitable for use in a spent nuclear fuel facility. The Äspö HRL provides a realistic and undisturbed research environment at a considerable depth and the knowledge gained will be used for the construction of a final repository that is due to be built in the coming years. Äspö HRL consists of buildings and laboratories on the surface and a network of tunnels below ground. The underground part of the facility extends from the Simpevarp peninsula to the southern part of the island of Äspö and the tunnels spiral down to a depth of 460 m, which is where numerous experiments take place. The TASS Tunnel is one of these tunnels (Swedish Nuclear Fuel and Waste Management Co, 2012). The layout of Äspö HRL and the location of the TASS Tunnel can be seen in Figure 1.

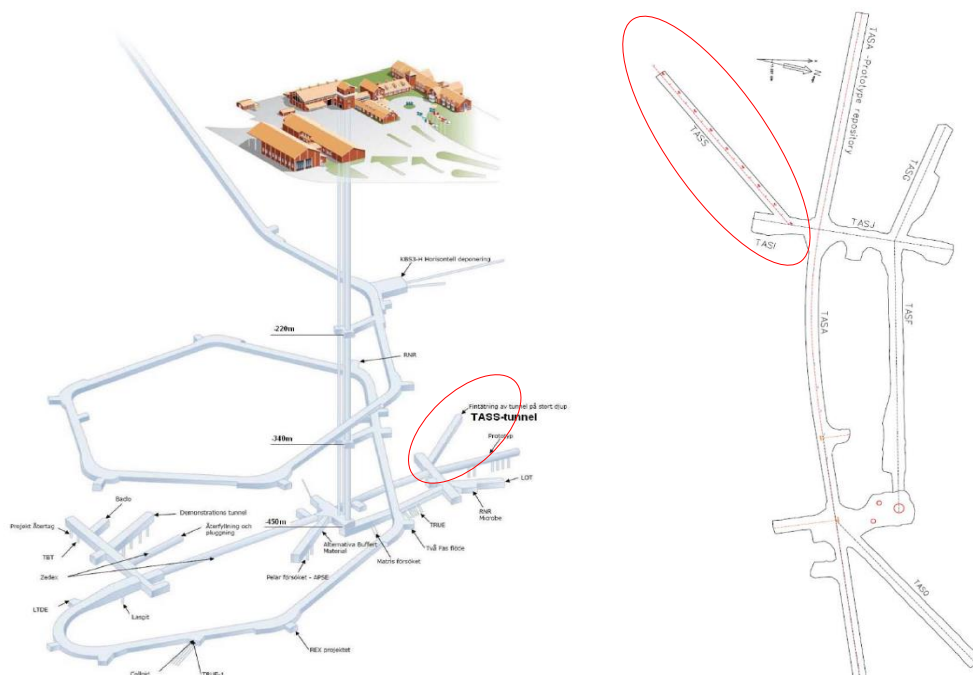


Figure 1. Location of the TASS Tunnel (Sigurdsson & Hardenby, 2010).

To carry out the necessary research on post-grouting performance, a small tunnel was excavated in the Äspö HRL facility. The project was entitled 'Sealing of a tunnel at great depth'. The project consisted of construction of a tunnel named TASS between October 2007 and December 2008, where pre-grouting and post-grouting methods could be studied. The tunnel was also used for a series of experiments to examine different types of explosives, borehole layouts and drilling techniques. The TASS Tunnel is located in an area where that fulfils a number of conditions, such as no or little interference with other activities. The tunnel orientation is perpendicular to the main water-bearing fractures and it is located outside the main drawdown of the groundwater table, i.e. there is no disturbance of the water level or head nearby. The direction of the TASS Tunnel is NE-SW, which is perpendicular to the main water-bearing fractures. The length of the TASS Tunnel is approximately 80 m, the theoretical tunnel area is 19 m² and it is 4.2 m wide and 4.8 m high (Sigurdsson & Hardenby, 2010).

1.3.2 Local geology

Sweden is part of the Fennoscandian Shield along with Norway, Finland and northwest Russia. The oldest parts of the Shield are estimated to be 2,500-3,100 million years old and are found northeast of the Kola Peninsula in Russia. The oldest rock in Sweden is Archaean rock, which can be found to a limited extent in northern Sweden, and is more than 2,500 million years old. In Sweden, there are three main components that make up the bedrock: Precambrian crystalline rocks, the remains of younger sedimentary rock cover and the Caledonides (Geological Survey of Sweden, n.d.). Sweden lies within three different provinces: northern and central Sweden belong to the Svecofennian province along with southwest Finland. The southern part of Sweden belongs to two provinces, the Transscandinavian igneous belt (TIB) and the Southwestern gneiss province.

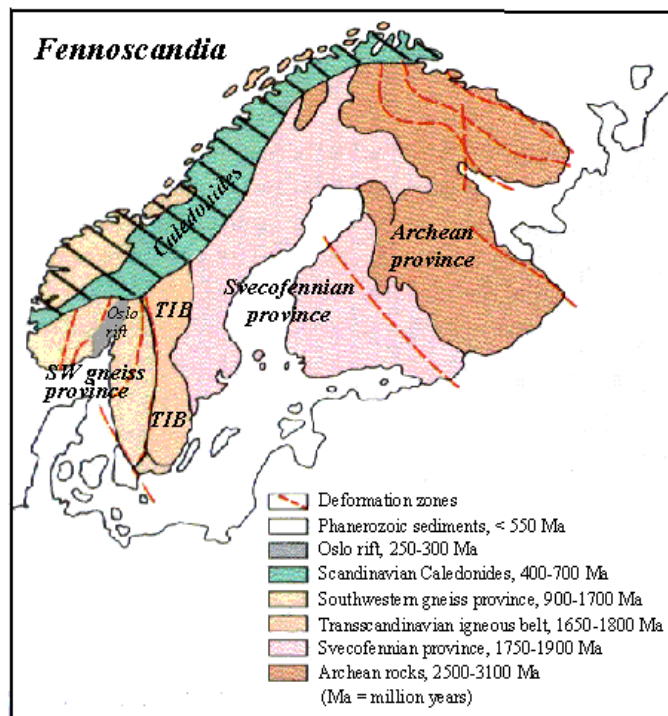


Figure 2. Fennoscandia Shield (Geological Survey of Sweden, n.d.).

Äspö HRL is located on the Transscandinavian igneous belt (TIB), which was formed 1,650-1,800 Ma ago. The belt extends northwards from Småland in southern Sweden and under the Caledonian mountain chain (see Figure 2). The composition of the TIB bedrock is mainly undeformed granitoids and associated porphyries, which were formed in at least three different phases during the period (Andersson, 2009).

The dominant rock type found in the TASS Tunnel is Äspö diorite, which makes up approximately 90% of the rock mass. Äspö diorite is commonly medium-grained and massive with white-pinkish feldspar megacrysts, 5-20 mm in size. The appearance of the rock is usually grey-dark grey. Other rock types that can be found are fine-grained granite, pegmatite, quartz veins/lenses, undifferentiated mafic rock and hybrid rock. Hybrid rock is bedrock that is a mixture of Äspö diorite and fine-grained granite (Sigurdsson & Hardenby, 2010).

1.3.3 Geological mapping of the TASS tunnel

The main reason for excavating the TASS Tunnel was to examine whether grouting compounds used could seal very deep tunnels that are subjected to high groundwater pressure. Complete geological mapping of the TASS Tunnel was carried out and published in the report *Äspö Hard Rock Laboratory – The TASS Tunnel – Geological Mapping* by Hardenby and Sigurdsson 2010. The report describes the geological features of the tunnel and briefly how laser scanning was performed.

When mapping stage 2 (20.7 – 48.7 m), which is where post grouting took place, it was found that Äspö diorite makes up 98% of the rock volume and therefore dominates this mapping stage. See Figure 3 for the location of the mapping stage. The rock quality of the mapped surfaces based on RMR (Rock Mass Rating) in the tunnel section was found to be 66, which is considered good rock (RMR = 61-80). The walls and roof together have a higher RMR value, 68. The RMR value of the floor is 58, which is considered to be fair rock (RMR = 41-60). The RMR system is an empirical classification system which combines the most significant geological parameters and represents them with one overall value of rock mass quality.

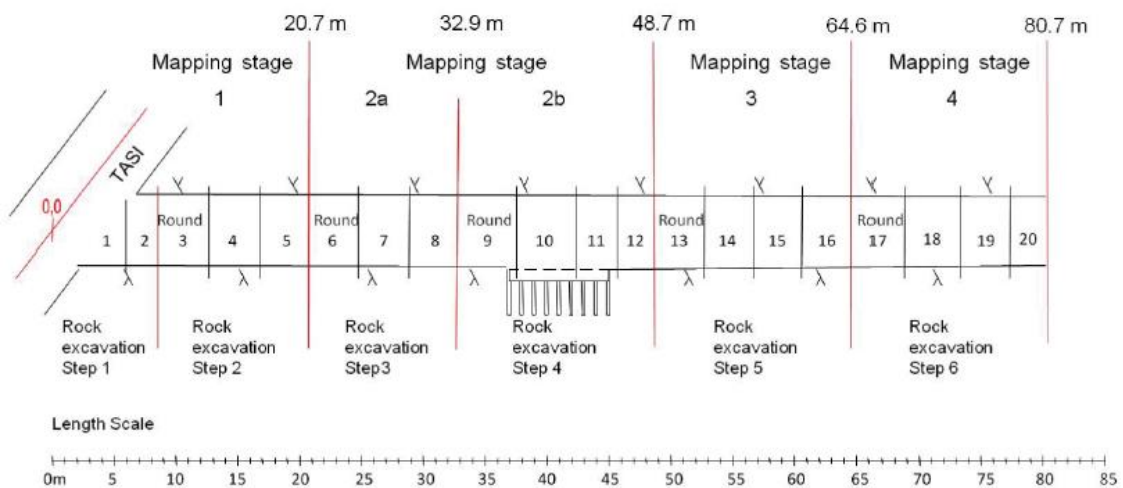


Figure 3. Mapping stage of the TASS Tunnel (Sigurdsson & Hardenby, 2010).

In the entire TASS Tunnel there are two main fracture sets: the dominating fracture set is east-west striking and steeply dipping. The set has a mean orientation of 097/86. The second fracture set can be divided into two sub-sets with mean orientations of 037/03 and 280/18. The set is sub-horizontal to gently dipping with a more varying strike. From the second mapping stage, three main fracture sets are apparent: major fracture set 1m: 285/27, major fracture set 2m: 094/87 and major fracture set 3m: 069/01, all of which coincide with the major fracture sets mapped for the entire tunnel. The orientation of all the fractures in the TASS Tunnel and fractures in the second mapping stage, presented in Schmidt net and joint rosette diagrams, can be seen in Figure 4.

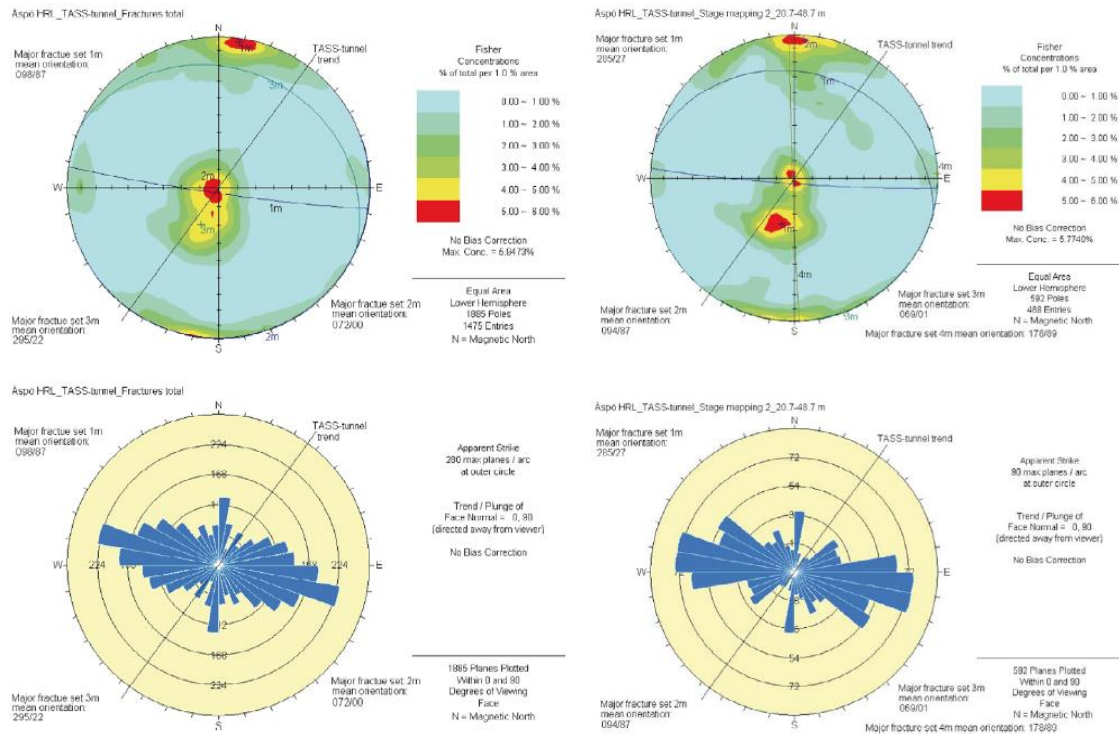


Figure 4. Schmidt net and rosette diagrams. Left: All the fractures mapped in the TASS Tunnel. Right: All the fractures mapped in stage 2 (20.7 – 48.7 m) (Sigurdsson & Hardenby, 2010).

One of the main areas of interest in this project is identification of the inflow into the tunnel. However, it should be noted that the geological mapping took place after the pre-grouting process. Mapping of water-bearing fractures therefore only shows fractures that have not been successfully grouted. Where possible, the inflow quantity was measured/estimated by counting drops of water. Mostly, the quantity was given in terms of moist, wet or flow by predefined method (Sigurdsson & Hardenby, 2010).

According to Figure 5, there are two distinct concentrations, showing sub-horizontal and gently dipping fractures. The main orientation sets are 1m: 289/27 and 2m: 131/01. There is also a less prominent set 3m: 289/85. The north-south trend is mainly caused by horizontal fractures with an orientation of 000/00. Two other less prominent water-bearing fracture sets were also discovered, with mean orientations of 287/70 and 099/89. The main fracture set discovered in the second mapping stage indicates sub-horizontal fractures that contribute most to the inflow. The orientation of the set is 000/00, which coincides with the sub-horizontal orientation of all water-bearing fractures in the entire tunnel. The orientation of all water-bearing fractures and the water-bearing fractures in the second mapping stage, presented in the Schmidt net and joint rosette diagrams, can be seen in Figure 5.

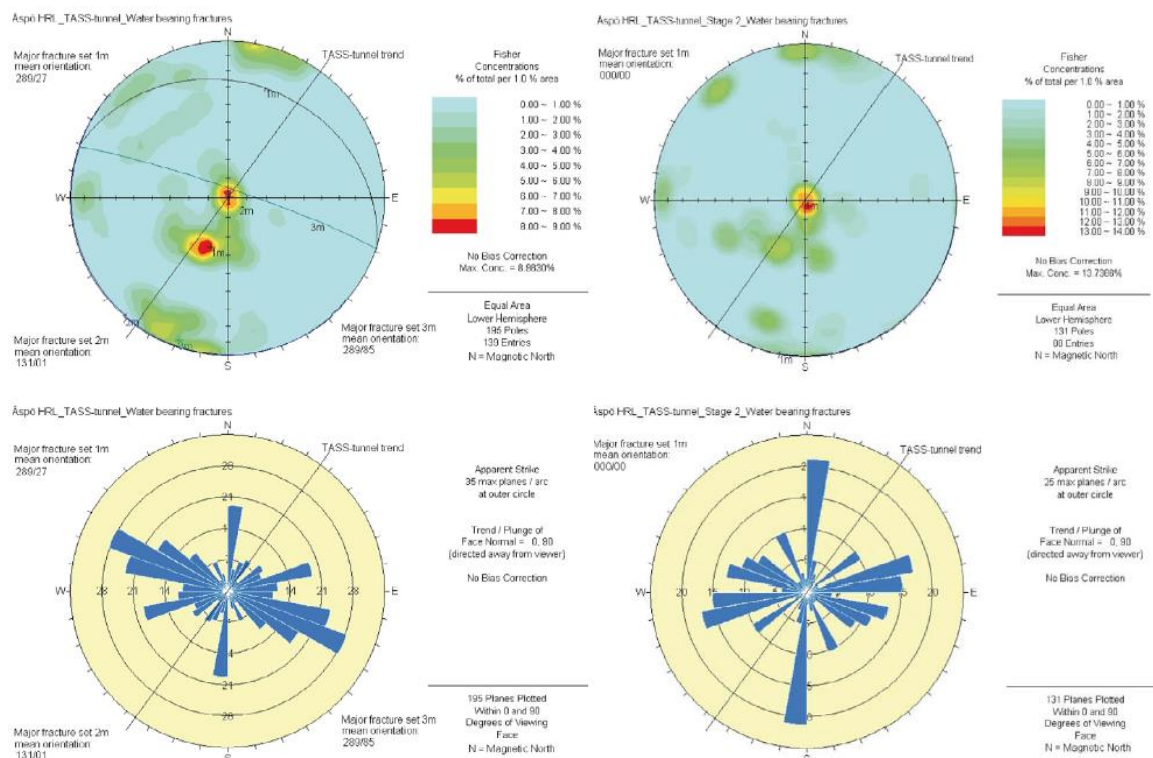


Figure 5. Schmidt net and rosette diagrams. Left: All the water-bearing fractures mapped in the TASS Tunnel. Right: All the water-bearing fractures mapped in stage 2 (20.7-48.7 m) (Sigurdsson & Hardenby, 2010).

1.3.4 Description of grouting layout

Even though the report focuses on post-grouting, it is necessary to describe the grouting layout for the pre-grouting process. Throughout the entire tunnel, six pre-grouting fans were drilled. Three of the fans extended outside the tunnel contour while two of them were inside the tunnel contour, see Figure 6. Pre-grouting took place inside the tunnel contour for section 34-50 m. After pre-grouting, the sealed zone was estimated to be only 1.5 m outside the tunnel contour, which is considered close (Funehag & Emmelin, 2011).

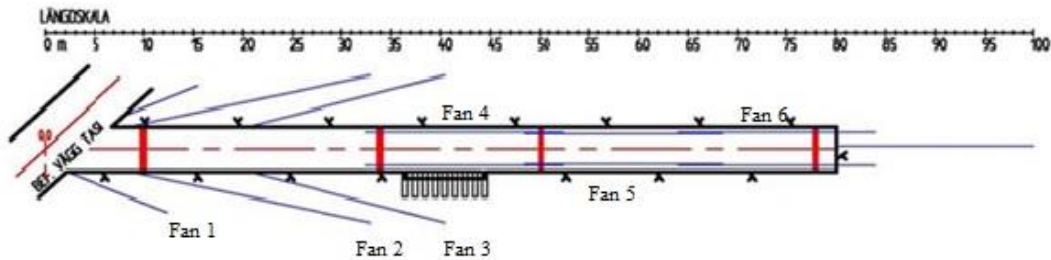


Figure 6. Plan view of the TASS tunnel with the pre-grouting layout. Fans 1-3 are outside the tunnel contour while fans 4-6 are inside the tunnel contour. Fans are labelled with blue lines (Funehag & Emmelin, 2011).

As stated earlier, post-grouting only took place in section 34-50 m because of unacceptable inflow. The post-grouting design was carried out by drilling grouting holes that were intended to seal the tunnel. These holes have either 'A' or 'B' added to their names. Between these grouting holes, special observation holes were drilled, designated control holes, which are denoted with a 'C'. The role of these holes was to monitor possible inflow and provide evidence that the previous grouting fans were sealed. Following this inspection, the control holes were also grouted.

The design of the grouting layout was as follows: a total of eight fans were installed, four in the tunnel ceiling and four in the walls and floor. The junction between the ceiling fans and the wall fans was set in order to reach up/down to the middle of the wall. This layout consists of eight boreholes in the tunnel ceiling and 12 boreholes in the walls and floor, see Figure 7.

Design of the control fans layout was as following: total seven fans were installed, four in the roof and three in walls and floor of the tunnel. The control fans consisted of 9 boreholes in the roof and 13 boreholes in walls and floor, see Figure 7.

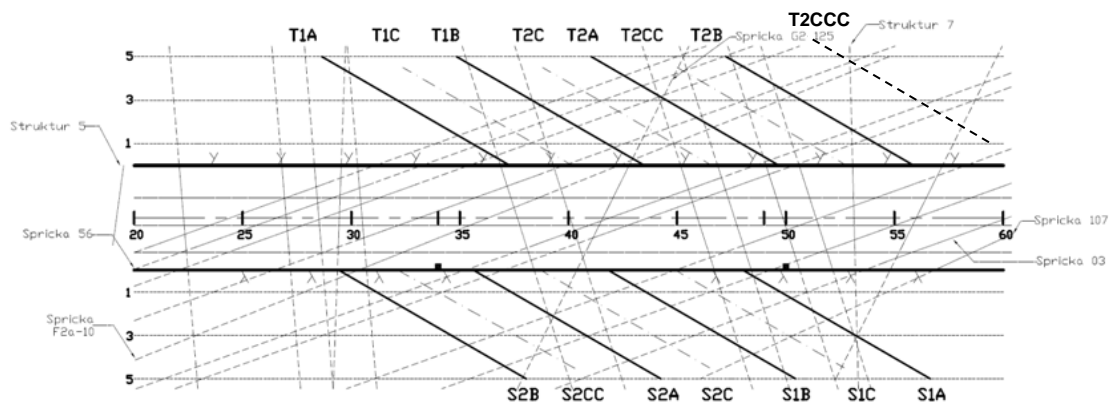


Figure 7. Geometry of post grouting fans (Funehag, Unpublished).

The drilling angle was set at 30 degrees from the tunnel wall and the length of the boreholes was either 10 m or 14 m. Boreholes located on the right-hand side of the tunnel were set at 14 m, viewed in the longitudinal direction of the tunnel. Boreholes with a length of 14 m were drilled for other experiments and they were also used as observation holes. The distance from the bottom of the borehole to the tunnel contour was found to be 5 m for borehole length 10 m and 7 m for borehole length 14 m. The spacing between the boreholes was set at 2.5-3 m to obtain a reasonable grouting time and to avoid spacing that was so dense that it could result in connected boreholes.

1.4 Methodology

Literature study will be carried out in order to compile knowledge of the geology, hydrogeology and grouting. Where fundamental facts and theories about these areas and how they are related and interact are presented. Successful grouting is achieved by knowing how these areas interact and their properties.

The geology is the fundamental area to examine before tunnel excavation. The data obtained from geological inspection before and after the excavation provide valuable information about the condition of the tunnel and what can be expected in terms of inflow. Knowledge about the hydrogeology is essential in order to obtain more detailed information about hydraulic gradient and water shear stress. By evaluating the borehole data, i.e. inflow and pressure data, it is possible to estimate the hydrogeological properties and make a rough estimation of the hydraulic gradient. A proper estimation of the hydraulic gradient can be done with regard to the geometry.

Grout properties and grouting procedure are also important in the overall estimation of grouting performance. Using the information acquired from the grouting performance, the shear strength of silica sol can be estimated. By knowing both the shear stress of water and the shear strength of silica sol it is possible to compare the values with the erosion criteria. A flow chart explaining the methodology for this project is presented in Figure 8.

The main aim of this report is to produce a hypothesis about why boreholes leak after post-grouting and with special attention given to possible erosion of silica sol due to high hydraulic gradients. With a thorough examination of how these areas interact, an

evaluation of data obtained before and after post-grouting, and an examination of the grouting performance, a hypothesis can be made.

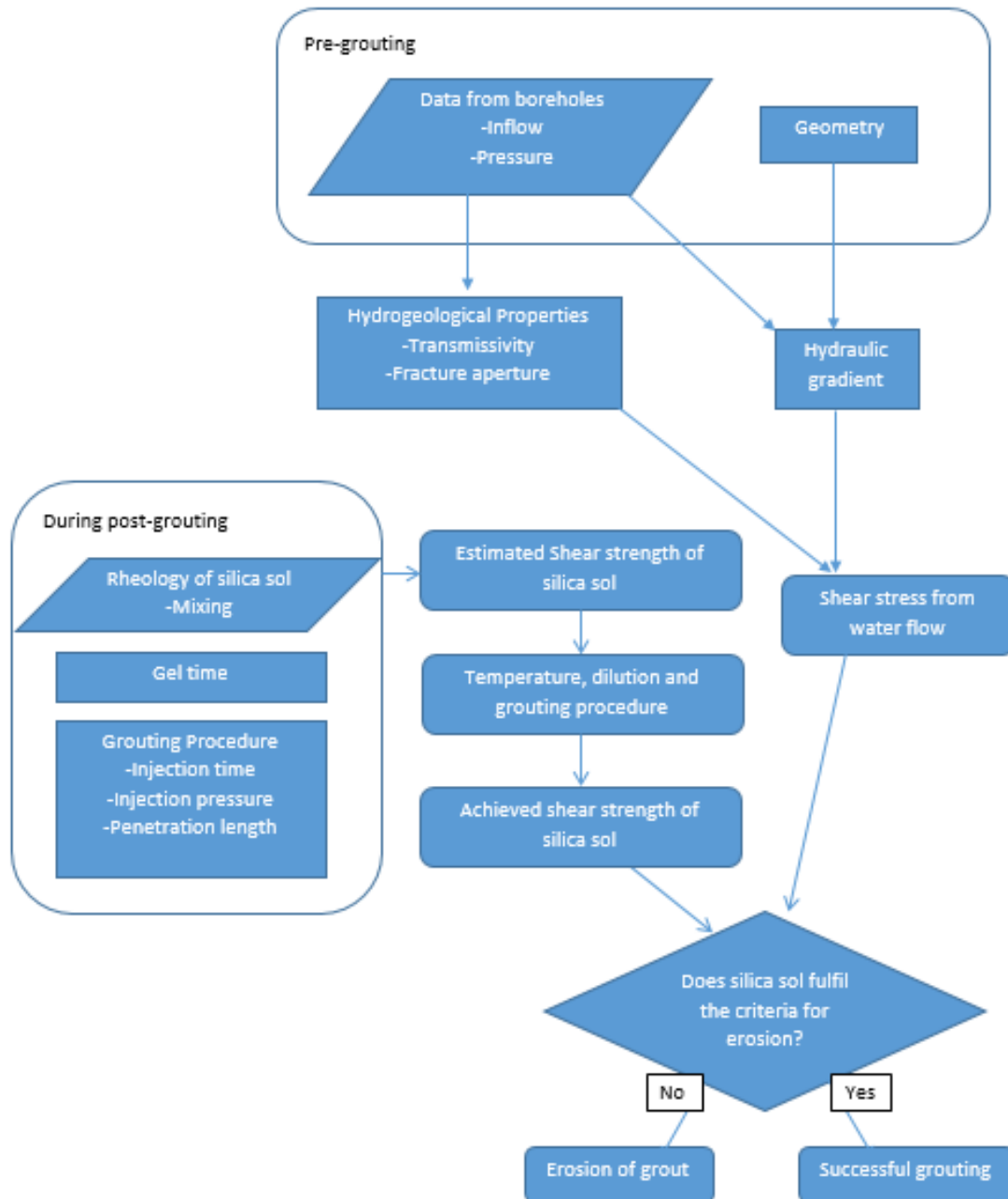


Figure 8. Methodology flow chart.

2 Theory

2.1 Geological mapping

Bedrock can be a complex structure that can be described using geological mapping. According to the Geological Survey of Sweden (SGU), it is necessary to map the bedrock to obtain a complete picture, with a description of the distribution, interrelationships, mineral composition, mode of formation and age of the different rocks, and to identify any structures present. How geological mapping is performed can vary between projects and applications. Information gathered from geological mapping can be used in construction projects, civil engineering projects, mining, working with environmental issues and various other applications. Through visual inspection of rock at the surface, which is called an outcrop, or examination of the drill core, it is possible to carry out geological mapping (Geological Survey of Sweden, u.d.). The mapping can also be carried out inside the tunnel through visual inspection of the rock after excavation.

During the geological mapping of the TASS Tunnel the following elements were registered (Sigurdsson & Hardenby, 2010):

- Rock types – Strength
- Rock boundaries/contacts
- Alteration
- Fractures
- Deformation zones
- Occurrence of water/water leakage
- Rock Mass Rating (RMR)

Data that can be used to characterise and analyse fractures can be obtained from the numbers and directions of the fractures, which can be measured from the surface or from drill cores. This data can be used for grouting design and strength/stabilisation purposes. Strike is the clockwise angle between north and the intersection between the horizontal plane and the fracture plane. Dip is measured as the inclination of the fracture plane, see Figure 9.

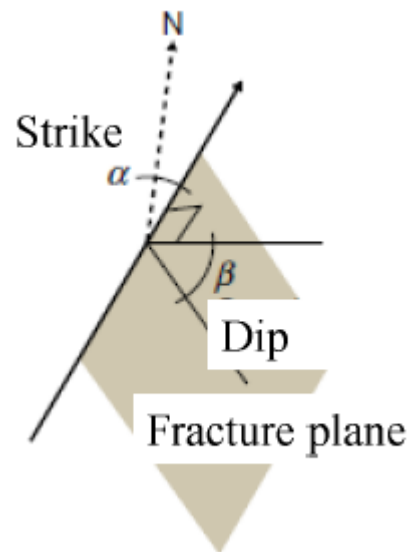


Figure 9. Definition of dip and strike.

To interpret the data visually, two methods are common: joint rosette diagrams and a Schmidt net. A fracture rosette is a way of showing the directions of the fractures. Dominating fracture sets are easily distinguished by dividing the fracture directions into classes, e.g. 5° intervals. Each class is then plotted on the fracture rosette. A fracture rosette does not show dip data. A better way of showing fracture data is to use a Schmidt net, where the normal to the fracture plane is projected onto a lower hemisphere, viewed from the crown of the upper hemisphere. Every fracture will therefore match a point projected on the circle that corresponds to the hemisphere and groups of points represent fracture sets (Gustafson, 2012).

2.2 Description of fractures in hard rock

One of the main components in Swedish bedrock is Precambrian crystalline rocks. These are normally igneous and metamorphic rocks, approximately 545 million years old (Geological Survey of Sweden, n.d.). Crystalline bedrock can be described as hard and fractured and the rock itself is dense and almost impermeable. The structure and properties of fractures are important in engineering, geoenvironmental and hydrogeology because of their ability to transmit groundwater flow. A system of fractures in the rock allows the groundwater to flow through the rock mass. The hydrogeology of crystalline bedrock consists mainly of describing the permeability through the fracture system.

A fracture can be described as mechanical breaks in the rock, caused by deformation in brittle rock formed in response to stress. In other words, fractures form and spread through the rock when stresses are equal to the rock strength (Gustafson, 2012). Swedish crystalline bedrock is very old and has therefore been subjected to various geological events that can cause fracturing. The origin of stress can arise from different events, such as the weight of the Earth's crust, high fluid pressure, tectonic pressure and thermal loading (National Research Council (NRC), 1996). The scale of fractures varies from microscopic to continental. The appearance of fractures and fracture zones cannot be explained easily and a variety of parameters can be used to describe the fracture appearance and the fracture zones (Gustafson, 2012).

In principle, groundwater flows through fractures that have the largest aperture, i.e. along lines of least resistance. The flow will therefore become uneven through fractures and be difficult to measure. Rock that contains fractures needs to have contact points between fracture surfaces to distribute the rock stress. The fracture therefore has an irregular structure and the aperture can vary along the fracture. These contact points normally occupy a small portion of the fracture plane and depend on the type of fracture and the rock stresses, which is a function of depth. Stagnant pores can be formed when small lateral joints become isolated from the fracture. These pores do not precipitate in the groundwater flow but can be involved in exchange with the groundwater through diffusion (Gustafson, 2012). It can also be expected that a fracture contains rock fragments; secondary minerals from the time a fracture was formed or reactivated, or precipitated minerals from flowing groundwater. During the trace element experiments (TRUE experiment) at Äspö HRL a conceptual model of water conductive fracture has been built (Winberg, et al., 2000), see Figure 10.

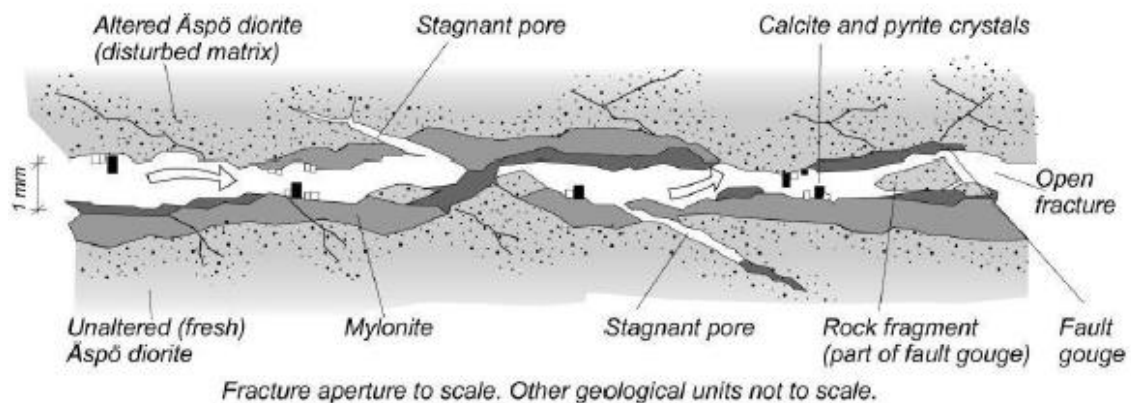


Figure 10. Conceptual model of water conductive fracture (Winberg, et al., 2000).

A fracture zone can be described as a zone where fracture frequency is at least ten times higher than the surrounding rock and is usually on one plane where the orientation can be expressed as dip and strike (Gustafson, 2012). The fracture zone represents a zone where major deformations have taken place and when zones are characterised by brittle failure, it is called a brittle deformation zone. Various types of fractures can be found in the fracture zone, including fractures where substantial shear deformation has taken place and where movement is almost impossible. These fractures are usually open.

It is common in fracture zones that a few of the fractures are responsible for most of the flow with other fractures containing water but contributing less flow due to low permeability. This can be a problem. When these large, water-bearing fractures are sealed during grouting, the flow will find smaller fractures and inflow problems remain (Gustafson, 2012).

2.3 Hydrogeology of bedrock

Hydrogeology can be described as the occurrence, distribution, movement and geological interaction of water in and above the Earth's crust, which is part of the hydrological cycle, i.e. continuous circulation of water above and below the surface of the Earth. This cycle contains three major pathways: precipitation, evaporation and vapour transport (surface water and groundwater flow) through terrestrial and atmospheric environments. Storage points for water can include ice caps, oceans, surface water, groundwater and the atmosphere. An exchange process between storage points is driven by the sun, with water being evaporated by heat from the sun, condensed into clouds, precipitated back to Earth and going straight to surface water flow or groundwater flow (Hiscock, 2005).

2.3.1 Fracture flow

Groundwater flow in rock differs from flows that occur in sediment, such as sand or gravel. The geometry and properties of fractures need to be described differently compared to pores in sand and gravel. Groundwater flow in porous and fractured rock can usually be assumed to be laminar. When the flow changes direction, inertia forces are formed but assuming that flow is laminar it is possible to disregard these forces (Gustafson, 2012). A result of this assumption is a linear relationship between flow through the rock and the required energy to drive the flow. This can be explained using Darcy's Law (Darcy, 1856) which in general terms describes flow through a porous medium, see Eq. 2.1.

$$Q = -K \cdot A \cdot \frac{dh}{dx} \quad \text{Eq. 2.1}$$

Where Q is flow through the cross-sectional area, A is the proportionality constant, K is the hydraulic conductivity of a porous medium that describes the ease of movement of water through a porous medium, and dh/dx is the hydraulic gradient. The negative sign of the hydraulic gradient indicates flow in the direction of a decreasing hydraulic head. Hydraulic conductivity for fracture flow can be expressed using Eq. 2.2.

$$K = \frac{\rho \cdot g \cdot b^2}{12 \cdot \mu} \quad \text{Eq. 2.2}$$

Where ρ is the density of water, g is the acceleration due to gravity and μ is the viscosity of water.

A common method to determine the hydraulic conductivity of the rock is to use a water pressure test (WPT test) (Emmelin, et al., 2007). During the test, water is injected into the borehole at constant pressure and for a limited period of time. Under assumed steady-state conditions, the injected water penetrates fractures connected to the borehole. The relationship between water quantity injected, injection pressure and transmissivity can thus be derived. Derivation can be seen in Gustafsson (2012).

In general, the characteristics of a fracture are difficult to describe. Performing hydraulic tests and evaluating the transmissivity is the most common way to describe a fracture aperture and the fracture network. This is done by simplifying the aperture of the fracture to a slit between two smooth parallel planes. Transmissivity, T , is directly proportional to horizontal hydraulic conductivity ($T = K \cdot b$) and is a measure of how much water can be transmitted horizontally. The relationship presented in Eq. 2.3, which is expressed using the cubic law (Boussinesq, 1868), can convert transmissivity, T , obtained from the hydraulic test, into a hydraulic aperture, b .

$$T = \frac{b^3 \cdot \rho \cdot g}{12 \cdot \mu} \quad \text{Eq. 2.3}$$

Hydraulic aperture can therefore be expressed using Eq. 2.4.

$$b = \sqrt[3]{\frac{12 \cdot \mu \cdot T}{\rho \cdot g}} \quad \text{Eq. 2.4}$$

A small change in the aperture size can have a big impact on the transmissivity. The mean velocity in the slot can be expressed using Eq. 2.5.

$$v_f = \frac{q_f}{b} = -\frac{dh}{dx} \cdot \frac{\rho \cdot g \cdot b^2}{12 \cdot \mu} \quad \text{Eq. 2.5}$$

Flow can be described as shearing of the material, where it will lead to movement or a flow. Accordingly, the fluid will apply a shear stress to the surroundings as it flows. The shear stress in a steady, laminar, 2-D flow between two planes is expressed using Eq. 2.6, with the assumption that the flow is the same across the slit and the fluid loses pressure due to the head loss over the length of the slit. Flow dimensions are described in the next chapter.

$$\tau = \frac{b \cdot g \cdot \rho}{2} \cdot \left(-\frac{dh}{dx}\right) \quad \text{Eq. 2.6}$$

In reality, fracture sides and surfaces are either flat or parallel and the fracture aperture and surface can fluctuate along the fracture. Flow in a fracture will have a tendency to

follow paths where there is least resistance and this has been reported by various researchers (Hakami, 1995) (Gale & MacLeod, 1990). These researchers describe the variation in the aperture in natural fractures and how the distribution of fracture apertures affects the transmissivity.

Research by Zimmerman and Bodvardsson (1996) describes the relationship between hydraulic fracture aperture and aperture. The relationship is expressed using Eq. 2.7.

$$b^3 = \langle a \rangle^3 \cdot \left[1 - 1.5 \cdot \frac{\sigma^2(a)}{\langle a \rangle^2} \right] \cdot (1 - 2c) \quad \text{Eq. 2.7}$$

Where the hydraulic fracture aperture is a function of the mechanical mean aperture, $\langle a \rangle$, the variance $\sigma^2(a)$, and the proportion of the closed fracture area. With a large value for the variation coefficient $\sigma(a)/\langle a \rangle$, the permeability of the fracture will be reduced considerably. With variation coefficient values higher than 0.8, a fracture will degenerate into a system of channels in the fracture plane. This also applies if the contact area c , approaches 0.5 (50%) and the hydraulic aperture therefore reaches a value of zero, implying that hydraulic continuity in the fracture ceases (Zimmerman & Bodvarsson, 1996).

2.3.2 Flow dimensions

In general, groundwater flow is only conducted through fractured rock and is therefore governed by the fracture geometry. To describe the hydraulic properties of the rock, analyses of the fracture geometry need to be performed. Flow dimension can be divided into the following conceptual models:

- 1-D flow (channel flow)
- 2-D flow (radial flow)
- 3D flow (rock is a homogeneous continuum)

One-dimensional flow (1-D flow) can be described as flow channelled into open channels. The reason for 1-D flow is that the fracture aperture varies across the fracture plane. This also applies to channels that are formed when two fracture planes intersect. 1-D flow in a fracture is illustrated in Figure 11.

Another way to characterise a fracture system is to use a conceptual model where fractures are described as two-dimensional and with a flat structure. The fracture is therefore described using its finite extent, l , and the fracture aperture, $a(x,y)$, which varies across the fracture plane. The groundwater therefore flows along the plane of the fracture and can be expressed by analogy to Darcy's law, where the relationship between flow in the fracture, q_f , per unit of aperture and the hydraulic gradient can be expressed using Eq. 2.8.

$$q_f = \frac{Q}{w} = T \cdot \frac{\Delta h}{\Delta l} \rightarrow -T \cdot \frac{dh}{dl} \quad \text{Eq. 2.8}$$

The hydraulic conductivity can be expressed as $K=T/b$ and the hydraulic effective value for the fracture aperture as b . The hydraulic effective value must be identified in order to link it to the transmissivity. 2-D flow in a fracture is illustrated in Figure 11.

The last model describes the rock as an equivalent continuum in three dimensions with the hydraulic conductivity K . All rock properties are therefore evened out to give effective values that are equal at each point and in each direction.

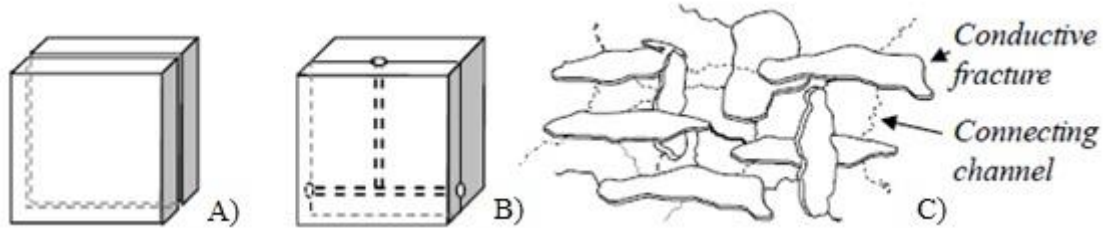


Figure 11. Conceptual models of flow in a fracture. A) Fracture with 2-D flow, B) Fracture with channelled 1-D flow, C) Combination of 1-D and 2-D (Hernqvist, et al., 2012).

2.3.3 Transmissivity distributions

For a short duration test, it is assumed that the transmissivity, T , is equal to the specific capacity, Q/dh . The transmissivity is also proportional to the cube of hydraulic aperture, b . This is expressed using Eq. 2.9 (Funehag, 2012).

$$\frac{Q}{dh} \approx T = \frac{\rho g b^3}{12\mu_w} \quad \text{Eq. 2.9}$$

Where ρ the density, g is the gravity and μ_w is the viscosity of water.

To describe the transmissivity distribution for individual fractures, data is needed to estimate the number of fractures that intersect the borehole and to obtain information about the distribution between them. It has been proved that Pareto distribution can be used where there are many small values and few large values (Gustafson & Fransson, 2005). For example, along a borehole in bedrock there are usually a large number of fractures with a small aperture and a small number of fractures with a large aperture. Using Eq. 2.10, the probability of the transmissivity, T , is lower than the section transmissivity, T_n , i.e. $P(T < T_n)$.

$$P(T < T_n) = 1 - \frac{(T_{max}/T_n)^k}{N + 1} \quad \text{Eq. 2.10}$$

Where T_n is the transmissivity with the number n in a size-sorted sample of the total number N and k is the Pareto distribution parameter. T_{max} is the transmissivity of the largest fracture. By plotting $\log(1-P(T < T_n))$ against $\log(T_n)$ and adding a line through the data points, Pareto distribution parameter, k , can be estimated as the slope of the line.

By using data from the pre investigation of the TASS tunnel necessary parameters needed in the Pareto distribution can be found (Funehag & Emmelin, 2011). From the observation borehole KI0010B01 the Pareto distribution parameter, k is equal to 0.52

which gives the ratio $T_{TOT}/T_{MAX} = 1.5$ (Gustafson, 2012). Maximum transmissivity from one fracture is therefore approximately 70% ($1/1.5 \approx 0.7$) of the total transmissivity. This can be correlated to the maximum inflow, i.e. maximum inflow from one fracture that intersects the borehole is 70% of the total inflow.

2.3.4 Hydraulic gradient and inflow to a tunnel

Groundwater flow is mainly driven by gravity and causes small pressure differences in undisturbed rock. Based on borehole transmissivity measurements performed by SKB at the Forsmark and Oskarshamn sites, it is estimated that the naturally occurring hydraulic gradient in undisturbed rock is generally far below 1 m/m (Nordquist, et al., 2008). However, when excavation is performed in rock, such as tunnels, it will cause pressure differences between the water in the surrounding rock and space with atmospheric pressure. The groundwater pressure around the tunnel will cause a hydraulic gradient towards the tunnel, the gradient expressing the loss of energy along the flow path in a groundwater flow. The gradient is expressed as $-dh/dl$ and is always considered negative since energy must flow from high to low. The energy is measured as a potential h , which physically is equal to the water table as expressed in Eq. 2.11.

$$h = \frac{p_w}{\rho_w \cdot g} + z \quad \text{Eq. 2.11}$$

Where p_w is the groundwater pressure, ρ_w is the water density and z is the depth.

The hydraulic gradient is defined using Darcy's law and is explained in Chapter 2.3.1. It should be noted that the gradient is a dimensionless unit (m/m).

High groundwater pressure close to the tunnel provides a high gradient. The gradient is also affected by whether the tunnel is grouted or not. Due to pre-grouting, it can be assumed that the largest apertures are sealed while the gradient acts in the smaller apertures that are not grouted. The hydraulic gradient is therefore transferred through the sealed zone in fractures that are not grouted. There is therefore full groundwater pressure outside the sealed zone while water pressure inside the tunnel is zero. The pressure difference over the sealed zone can therefore be significant. Figure 12 shows possible pressure scenarios for different grouting condition. These conditions are described as following:

- The tunnel has been pre-grouted with high sealing efficiency. The sealed zone is relatively thin and high pressure difference is acting over the zone. Very high hydraulic gradient is likely to act over the sealed zone. This can lead to problems during post grouting since high hydraulic gradient is acting in remaining fractures (Axelsson, 2009).
- The tunnel has been pre-grouted with low sealing efficiency. The sealed zone is relatively thin and the pressure difference acting over the zone is smaller than for good sealing efficiency.
- The tunnel has been pre-grouted and also post-grouted, the sealing efficiency is therefore high. It is assumed that the tunnel has previously grouted with low

sealing efficiency. The pressure difference is therefore high over pre- and post-grouted zone.

- The tunnel is not sealed. The tunnel acts as a drainage where atmosphere pressure acts inside the tunnel and groundwater pressure is static far from tunnel wall. For all of the cases it shall be noted that the rock is assumed to be homogenous, or highly fractured.

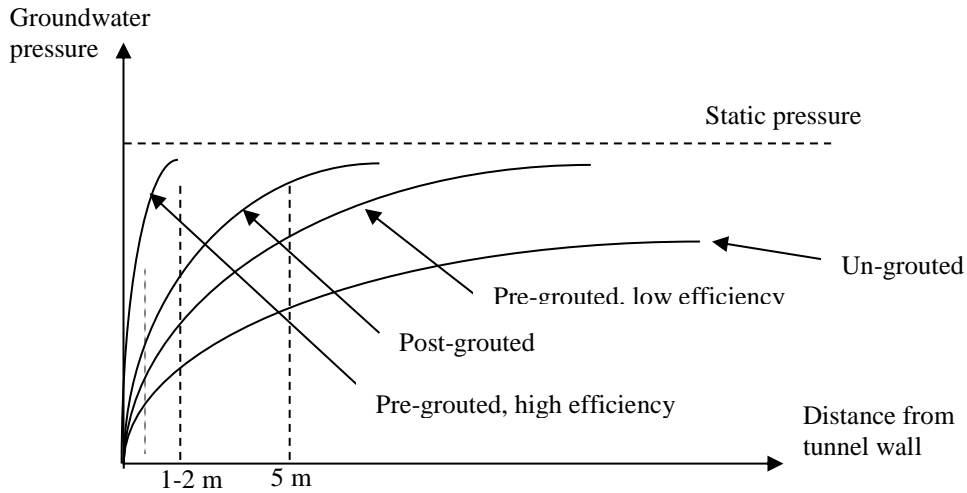


Figure 12. Pressure differences over different grouting scenarios.

Inflow into a pre-grouted tunnel can be expressed using Eq. 2.12, which is based on Hawkins (1956):

$$Q_T = \frac{2\pi \cdot T_0 \cdot H}{\ln\left(\frac{2H}{r_t}\right) + \left(\frac{T_0}{T_{inj}} - 1\right) \cdot \ln\left(1 + \frac{t}{r_t}\right) + \xi} \quad \text{Eq. 2.12}$$

Where Q_T is the inflow into the tunnel per length, T_0 is the transmissivity of the undisturbed rock, T_{inj} is the transmissivity of the grouted zone, H is the groundwater head, L is the length of the tunnel section, r_t is the tunnel radius, t is the thickness of the grouted zone and ξ is the skin factor.

The gradient that acts around the grouted tunnel can be expressed using Eq. 2.13 (Funehag & Emmelin, 2011).

$$-\frac{dh}{dr} = \frac{Q_T}{2\pi \cdot T_{inj} \cdot r} \quad \text{Eq. 2.13}$$

By combining Eq. 2.12 and Eq. 2.13 the gradient that acts around the tunnel can be expressed using Eq. 2.14.

$$-\frac{dh}{dr} = \frac{H}{r} \cdot \frac{T_0}{T_{inj}} \cdot \frac{1}{\ln\left(\frac{2H}{r_t}\right) + \left(\frac{T_0}{T_{inj}} - 1\right) \cdot \ln\left(1 + \frac{t}{r_t}\right) + \xi} \quad \text{Eq. 2.14}$$

The gradient at the tunnel wall can be calculated by setting the radius, r , equal to the tunnel radius. The radius is $r = r_t + t$ at the outer face of the grouted zone (Funehag & Emmelin, 2011). The gradient around an un-grouted tunnel can be expressed using Eq. 2.15. The maximum value of the gradient is therefore located next to the tunnel wall since $r \approx r_t$. Furthermore, the transmissivity of the rock and the transmissivity of the grouted zone are equal, $T_0 = T_{inj}$.

$$-\frac{dh}{dr} = \frac{H}{r} \cdot \frac{1}{\ln\left(\frac{2H}{r_t}\right) + \xi} \quad \text{Eq. 2.15}$$

A reduction in the transmissivity in the grouted zone increases the hydraulic gradient over the zone, i.e. this will lead to a high hydraulic gradient in the remaining fractures through the grouted zone. Since most of the hydraulic gradient is taken up through the sealed zone, the hydraulic gradient outside the sealed zone in the ungrouted rock will decrease. Post-grouting performed behind the grouted zone will therefore face a lower gradient and is more likely to succeed. However, the high hydraulic gradient acting on the un-grouted fractures in the sealed zone must be taken into account due to the risk of erosion. Schematic figure where post grouting is explained can be seen in Figure 13.

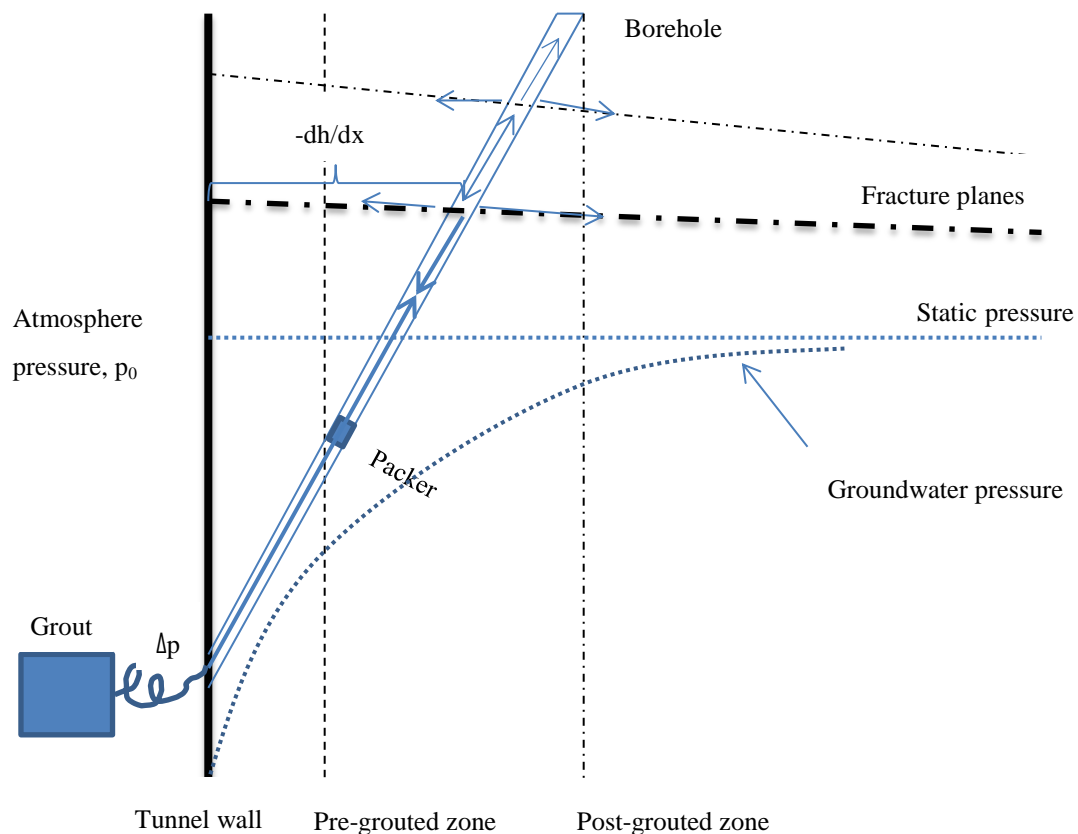


Figure 13. Schematic figure of post grouting.

The description of the hydraulic gradient is based on a continuum model and fractured rock can be described as anisotropic. The actual distribution of the hydraulic gradient is complicated to describe. The best approximation of hydraulic gradient towards a tunnel can be made by measuring the hydraulic head in a borehole and assuming that the head

is acting across the fracture length from the borehole to the tunnel wall (Axelsson, 2009).

2.4 Grouting

The main reason for grouting is to reduce or stop movement of water and/or strengthen the formation (Warner, 2004). Understanding the characteristics of the rock mass is therefore important in grouting design. Grouting involves filling fractures, joints and other faults with cementitious or chemical grouts to block the flow path of the water. The most important properties of the rock mass need to be considered before grouting design takes place. Based on the following properties, a theoretical design can be chosen (Emmelin, et al., 2007).

- Transmissivity (specific capacity) and hydraulic aperture.
- Fracture frequency, orientation and connections between fractures.
- Hydraulic head, hydraulic gradient and rock stresses.

Pre-grouting is a common method used to seal underground constructions where the grouting takes place before excavation. However, in some cases pre-grouting is not sufficient to meet inflow requirements and additional treatment, known as post-grouting, is necessary where grouting take place after excavation. Post-grouting will then take place where necessary to reduce the inflow after excavation.

Pre-grouting is usually performed in boreholes that lie in a fan shape around the tunnel front and takes place before excavation. The grout is injected into the boreholes under pressure to overcome the groundwater pressure. The grout will therefore be injected into the boreholes and into fractures intersecting the grouting boreholes, see Figure 14.

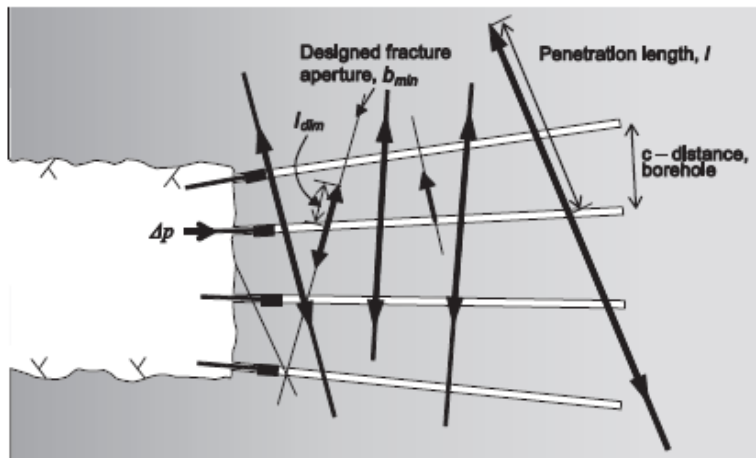


Figure 14. Model of the grouting procedure (Funehag, 2012).

The grout also needs to be sufficiently stable to withstand the forces from the flowing groundwater (Axelsson, 2009). The grouting process is therefore an interaction between the following parameters (Funehag, 2007):

- The rock mass: Minimum hydraulic aperture, b_{min}
- The grout: Viscosity, μ_0 , yield stress, τ_0 , and gel time, t_G
- The technique: Pressure, Δp , and efficient time, t

To achieve a good seal around the tunnel, it is necessary to choose grouting material with a good penetration length for given conditions and a suitable injection pressure to overcome the groundwater pressure. Penetration length, I , must be sufficient to overlap grout from neighbouring boreholes. In other words, grout must fill the entire distance, L , between boreholes. A further description of penetrability and penetration length can be found in Chapter 2.4.3.

In general, post-grouting is a similar process to pre-grouting, the main difference being that the grouting takes place after excavation when the inflow requirement has not been met and a higher hydraulic gradient can be expected. A common method of designing the pre-grouting fan layout is to drill the borehole in a fan shape around the tunnel contour. The pre-grouting layout can also be inside the tunnel contour. This method, however, will result a thin sealed zone compared to the fan-shaped layout. Post-grouting fans are therefore placed between pre-grouted fans or through the sealed zone to improve the existing low-permeable zone around the tunnel. Post-grouting is usually done with chemical grouting material such as silica sol since chemical grout is better at filling narrow fractures that are not likely to be filled using cementitious grout (Funehag, 2007).

However, it is known that grouting will never succeed completely for a number of reasons (Gustafson, 2012). The first reason is that certain fractures are too small for grouting material to penetrate. This applies especially to cement-based grout. The fine cement-based grout available on the market today is able to penetrate fracture apertures as narrow as 0.1 mm whilst chemical grout such as silica sol can penetrate fracture apertures as narrow as 0.01 mm (Funehag, 2007). If the grouting material does not penetrate properly into the aperture fractures it will result in non-grouted gaps between the boreholes.

The fracture system in the rock is usually a complex system and the route between boreholes is much more complex than a straight route. This can lead to underestimated penetration length (Gustafson, 2012).

The grouting process is usually carried out in the following order (Dalmalm, 2004):

- Drilling
- Cleaning
- Water loss or inflow measurement, where applicable
- Grouting
- Hardening of the grout
- Control holes drilled where applicable
- Water loss or inflow measurements
- Hole filling where applicable

Grouting boreholes are drilled with a certain distance between them and in a fan shape to obtain grout overlap between surrounding boreholes and thus a tight shield around the tunnel. It is also important to adjust the layout of the fans according to the orientation of the fractures in order to be sealed (Funehag, 2012). Cleaning of the boreholes is also an important step to flush out loose rock fragments formed during drilling (Axelsson, 2009). These fragments could have a negative effect on the grout characteristics and the injection of the grout and block the fracture entrance. In order to

ensure good mixing, it is necessary to measure the grout properties before injection. Parameters such as pressure, flow and volume as a function of time are then checked to see if they fall within pre-defined values (Fransson, 2008). Flow data can be used to identify the flow dimension and it can also indicate deformation and jacking during the grouting process (Gustafson & Stille, 1996). Performance is evaluated by measuring the inflow after grouting. This can be done using control boreholes or across a tunnel section using measuring weirs (Axelsson, 2009).

2.4.1 Silica Sol

Silica sol is a colloidal silica mixture, a low-viscosity aqueous dispersion of discrete particles (colloids) of amorphous silicon dioxide with the chemical formula SiO_2 (quartz). The particles are insoluble in water due to their hydroxylated surfaces and the diameter of colloidal silica is in the range 1-500 nm (Björnström, et al., 2003). During the manufacturing of colloidal silica, it is possible using controlled techniques to narrow the diameter range and create a more specific surface (Funehag, 2007). It is also a well-known compound used in industry for various applications, such as a cohesive agent for various fireproofing materials, for coating, for use as a catalyst and for use in the textile industry. Silica sol is also known in chemistry as nano-silica, colloidal silica or silica gel. There are numerous advantages of using silica sol as a grouting material. It is odourless, tasteless and non-toxic and it is therefore environmentally friendly (Broadchem Industrial, 2005).

When using silica sol as a grouting material, it is necessary to mix colloidal silica with salt; NaCl or NaCl_2 are usually used. At a predictable time this mixing will allow the particles to aggregate and form a strong, solid gel. The addition of more salt will make the gel form faster (Funehag, 2007). When the gel starts to form or the particles start to aggregate, a network of silica particles builds up and traps water molecules inside the network. Destabilisation of the sol occurs due to the presence of positive ions (Na^+ and Ca^{2+}) and a pH value in the range 7 to 10 and causes the silica particles to collide and form a network. It has good sealing properties and seals fractures that cannot be sealed using a cement-based grout.

In general, cementitious and chemical grouts can be described using the following properties:

- Flow properties (rheological properties).
- Penetrability properties.
- Gelling (curing) properties
- Bleed

Bleed describes the separation of water and the binding material in the grout. Bleed is not an issue for silica sol since the particles are of colloidal size. However, if silica sol is used in a dry environment, shrinkage can occur. Flow and penetrability properties will be presented in the following chapters.

Grouting in a fractured rock is always subject to uncertainties since a deterministic description of fracture zones is very difficult. If the injected silica sol were to hit a large, water-bearing fracture, dilution of the grout is likely to occur (Holmboe, et al., 2011).

This scenario is likely to affect the grouting procedure with a decreasing aggregation rate and an increasing gel time. During grouting, the gel time would need to be observed regularly until gelling has been achieved. The gel time can be determined using the beaker test. Gel time is achieved when the silica sol has a straight surface when the beaker is tipped 90 degrees (Funehag, 2012). The surface does not need to be entirely vertical although it does need to be straight. An illustration of the beaker test can be seen in Figure 15.

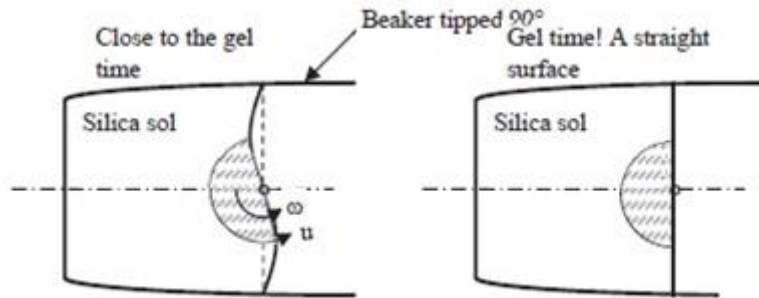


Figure 15. The beaker test is used to determine the gel time of silica sol (Funehag, 2012).

When grouting takes place in a borehole with a downward incline, water is likely to accumulate and dilute the silica sol during the grouting process. The water that remains in the borehole is mixed with the silica sol and becomes slurry (Funehag, 2012). It is likely that the accumulated water will dilute the saline solution and cause a lower ratio between the silica sol and the saline solution, resulting in a longer gel time. To avoid possible dilution, it is important to pump the remaining water out of the borehole before grouting takes place. However, water can still accumulate between pumping and commencement of injection.

2.4.2 Rheology and strength of Silica Sol

To describe the flow of grout in a fracture it is important to know the rheology of the grouting material. During the flow of a liquid, shear stress acts to resist the movement and cause internal friction in the opposite direction of the flow (Funehag, 2007). This behaviour is better known as viscosity and the internal friction makes it notable. The shear stress, τ , of a Newtonian fluid can be expressed using Eq. 2.16 where μ is the viscosity and $\dot{\gamma}$ the shear rate.

$$\tau = \mu\dot{\gamma} \quad \text{Eq. 2.16}$$

The grouting design is dependent on the material properties of silica sol, which consist of the gel induction time and the initial viscosity. The gel induction time, t_G , is the time at which the initial viscosity has doubled. For silica sol, the initial viscosity is approximately 5 mPas (Funehag, 2007). In general, a Newtonian fluid such as silica sol has a very low initial viscosity, which is constant and changes slowly. However when silica sol starts to form gel the grout will acquire the properties of a Bingham fluid, the step between Newtonian and Bingham fluid is difficult to determine (Funehag, 2012). Figure 16 illustrate the difference between a Bingham and Newtonian fluid. However, the advantage of Newtonian fluids is a rapid increase in viscosity and a rapid increase in strength compared with Bingham fluids. Gradual hardening of grout is called curing.

Traditional cement-based grout cures slowly while in the case of silica sol it is determined by the amount of saline solution used.

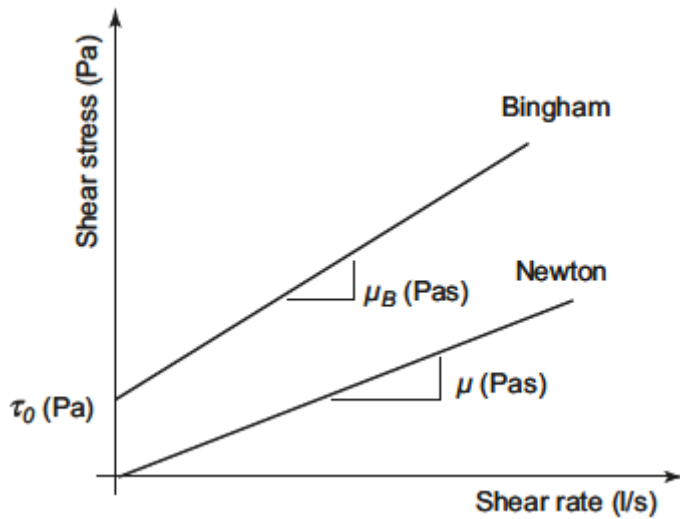


Figure 16. Rheological difference between Newtonian fluid and Bingham fluid.

The viscosity of silica sol can be determined using the mixing ratio between the silica sol and the saline solution; the lower the ratio, the faster the viscosity (Funchag & Axelsson, 2003). When viscosity is low, the penetration velocity is high. The velocity slows down significantly when the viscosity increases. This can be seen for four different ratios in Figure 17.

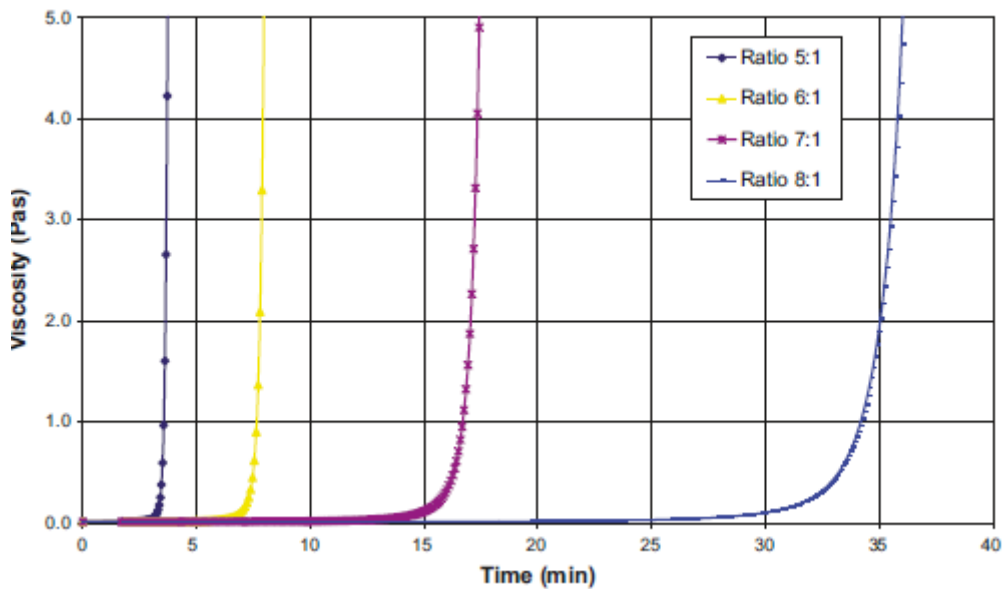


Figure 17. Viscosity behaviour of silica sol mixed with saline solution for four different ratios at 8°C (Funchag & Axelsson, 2003)

The hardening process of silica sol can be divided into four steps (Björnström, 2005):

- The first step occurs quickly. Particles start to merge and form chains when the saline solution is mixed with silica sol. This process occurs due to the charge-induced aggregation of the particles.

- Silica particles start to share hydrogen bonds and capture water. The captured water can be divided into bulk and wetting water. Bulk water consists of water molecules that interact with each other and wetting water bonds strongly with OH groups that are located on the silica particles. With increased temperature and low humidity during this phase there is a risk that the bulk water will evaporate. If evaporation occurs during this phase, the silica sol dries up and becomes dewatered. It is expected that silica sol will absorb water.
- In step three, bonds between silicon and oxygen start to form a very strong material based on Si-O-Si interaction. The hardbound water is then released.
- In the final step, irregularities are smoothed out when the top of the molecules begins to move towards the middle of the chains. This happens either due to a process called Oswald ripening or continued silica and oxygen attraction.

According to results from Axelsson (2009), the strength of silica sol increases over a long period and is relative to the humidity and temperature. The strength of silica sol will increase rapidly with decreased humidity and increased temperature. In the study it was shown that the shear strength of silica sol immersed in water after one day was in the range 5-10 kPa and 15-30 kPa after 30 days, see Figure 18.

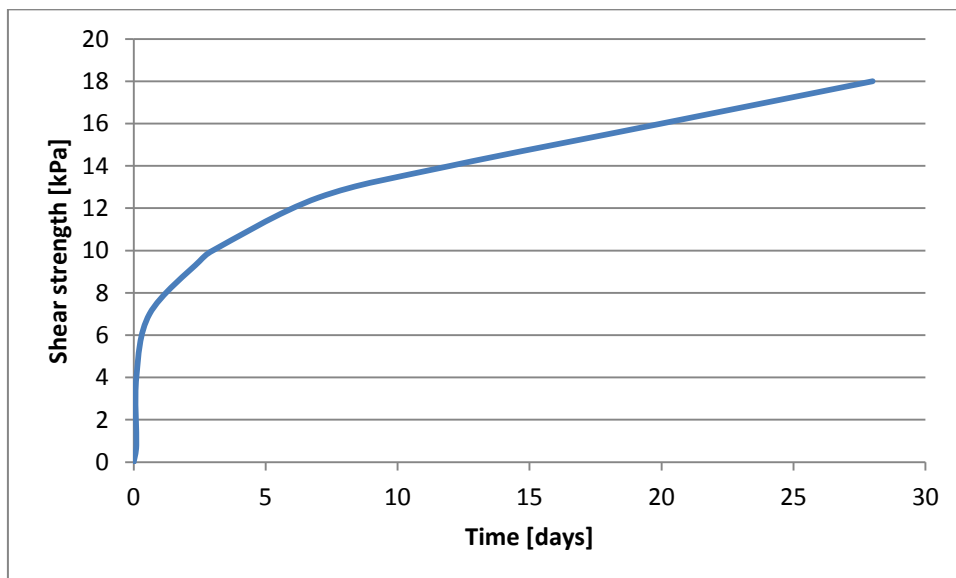


Figure 18. Strength development of silica sol immersed in water. Modified and redrawn from Axelsson (2009).

In Figure 19 from Axelsson (2008) development of early strength of Silica Sol is presented. The early shear strength of silica sol was determined by measurements with fall-cone equipment before gelling. The fall-cone test was performed by a cone with the weight 10 g and an angle of 60°. With these settings cone is able to measure the lowest strength possible, the measurement limit is approximately 60 Pa. To determine early shear strength that occur under 60 Pa limits an extrapolation were performed. According to Figure 19 shear strength is approximately 1 Pa after 40 – 50% of the gel time, which is sufficient for tunnels at moderate depths (~50 m). With increased depth the required grouting time increases, after 80% of the gel time the strength is approximately 50 Pa (Axelsson, 2009).

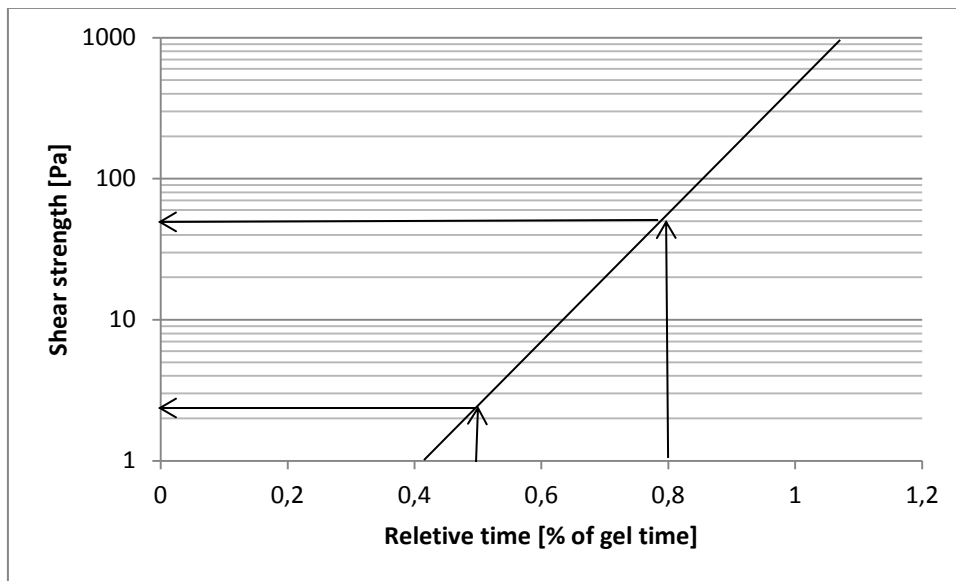


Figure 19. Development of early strength of silica sol. Modified and redrawn from Axelsson (2009).

The gelling formation of the silica sol depends to a large extent on the temperature. A simple rule of thumb for estimating the gelling process is that the gel time is halved if the temperature is doubled (Funehag, 2012).

2.4.3 Penetrability and penetration length

To determine the penetration length for grouts, the flow behaviour needs to be known. This behaviour can be described using a rheological model of the grout. The penetration length for Newtonian fluids such as silica sol depends on the viscosity development during gelling. According to Eq. 2.17, the penetration length for initial viscosity can be determined in 1-D flow, where the time taken for the velocity to double is taken into account, i.e. the gel induction time, t_G (Funehag, 2007).

$$I_{1-D} = b \cdot \sqrt{\frac{\Delta p \cdot t_G}{6\mu_0}} \quad \text{Eq. 2.17}$$

For 2-D flows, the penetration length is approximately 0.45 times the penetration length for 1-D flow according to Eq. 2.18 (Funehag, 2007). To use this equation, it is also necessary to know the fracture aperture, b , and the grouting overpressure, Δp .

$$I_{max,2-D} = 0.45 \cdot b \cdot \sqrt{\frac{\Delta p t_G}{6\mu_0}} \quad \text{Eq. 2.18}$$

With good distribution of grout in fractures, overlap between boreholes and fans will be ensured and sealing around the tunnel established. As a rule of thumb, the maximum penetration is achieved at half the gel time (Funehag, 2012). This grouting time is enough for shallow tunnels, <100 m. However, for tunnels at greater depths, 150-500 m there is higher risk of erosion due to high gradient and therefore should grouting time be longer to increase the grouts shear resistance when ending the grouting (Funehag, 2012).

To minimise the risk of high hydraulic gradients at large depths, it is important to have the sealed zone sufficiently grouted and achieve a good overlap between grouting fans. It is also important to ensure complete filling in each borehole to avoid backflow. Water is an incompressible fluid and can therefore have a maximum pressure equal to the grouting pressure. Air, however, is compressible and can be compressed to a very high pressure, resulting in a high risk of grout being driven out of the borehole after the packer is released (Axelsson, 2009).

To achieve good penetration and sealing effect, the geometry of the grouting fans needs to be considered. A common method is to drill the grouting holes in fans that lie around the tunnel contour. This is done by drilling into the tunnel contour at a certain angle and allowing the surrounding fans to overlap. The borehole angle will determine the thickness of the sealed zone. The sealing effect is also dependent on the distance between the boreholes. The distance is based on achieving a certain overlap of grout penetration between the boreholes. A schematic illustration of typical fan geometry outside the tunnel contour can be seen in Figure 20.

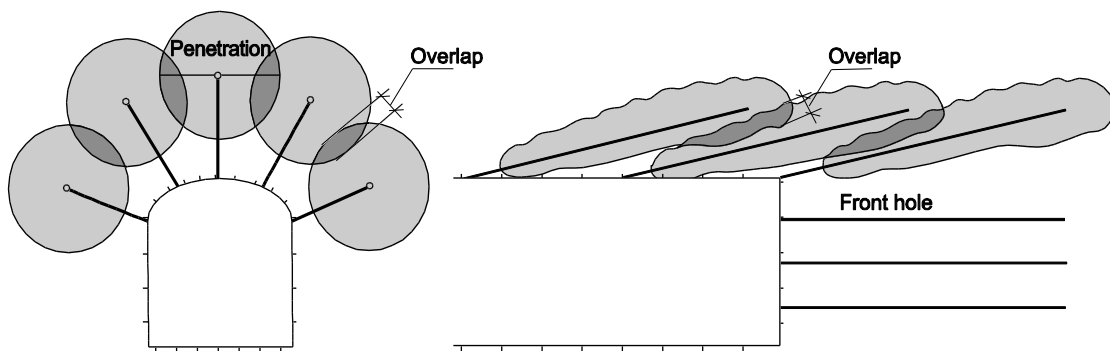


Figure 20. Schematic illustration of the geometry of grouting fans outside the tunnel contour. (Funehag, 2012).

Another grouting method is to drill fans inside the tunnel contour. By drilling boreholes inside the tunnel contour it is possible to avoid interruption in the rock by the boreholes. However, using this method the thickness of the sealed zone outside the tunnel contour will be less than if the previously described method is used.

2.4.4 Grouting pressure and flow

To achieve successful grouting and good distribution of the grouting material, the grouting pressure, grout flow and grouting time need to be considered.

Grouting pressure and flow are parameters that work closely. Increased pressure will produce an increase in flow. This is important when grouting takes place. Where there is a high water flow, the grouting pressure needs to overcome the existing groundwater pressure so that grouting can take place successfully. By using high grouting pressure a longer penetration length will be achieved and reduce the risk of backflow. The risk of fingering is also reduced with high pressure (Axelsson, 2009). A longer penetration length will also decrease the hydraulic gradient and thus the risk of erosion when grouting ends. It is important to apply grouting pressure that is lower than the minimum rock stress in order to avoid possible jacking of critical joints (Gustafson & Stille, 1996).

2.5 Erosion

In general, erosion in grouting holes can be described as the process where the shear stress from the flowing water exceeds the resistance of the existing grouting material and causes mechanical breakdown of the grout. There are three main processes that can cause this breakdown (Axelsson, 2009).

- Erosion - There is risk of erosion if water can flow where there is fresh grout. However, the shear stress of flowing water needs to exceed the shear strength of the grout. It is therefore important to have a higher shear strength for the grout to resist the erosion (Kutzner, 1996), (Nonveiller, 1989) and (Pusch, 1983).
- Fingering - When grouting take place, grout is supposed to replace the existing water in the fractures. This process can also do the opposite and allow water to replace the grout. This can occur if the difference in viscosity or pressure is too low, causing fingers of water to enter the grout. The risk of fingering can be reduced by choosing sufficient grouting pressure and grout viscosity (Andersson, 1998).
- Backflow - If adhesion between the rock and the grout is lower than the existing water force, a backflow can occur, i.e. when the bond between rock and the grout breaks in a fracture or/and in a grouted borehole (Axelsson, 2006). To avoid backflow in a fracture, the following criteria can be used, (Fransson & Gustafson, 2006).

$$I_D > \frac{p_w}{\Delta p} \quad \text{Eq. 2.19}$$

Where I_D is the relative penetration, which is dimensionless and in principle not a function of the fracture aperture. Note, this equation is only valid for grouts behaving as Bingham flow and exhibits shear strength such as cement grouts. Relative penetration is expressed by Eq. 2.20.

$$I_D = \sqrt{\theta^2 + 4\theta} - \theta \quad \text{Eq. 2.20}$$

The relative penetration is dependent on the flow dimensions. 1-D and 2-D flow are expressed using Eq. 2.21 and Eq. 2.22.

$$\theta_{1D} = \frac{t_D}{2(0.6 + t_D)} \quad \text{Eq. 2.21}$$

$$\theta_{2D} = \frac{t_D}{2(3 + t_D)} \quad \text{Eq. 2.22}$$

Where t_D represents the relative time expressed using Eq. 2.23.

$$t_D = \frac{t \cdot \tau_0^2}{6\mu_g \cdot \Delta p} \quad \text{Eq. 2.23}$$

Back-flow can also occur if the packer is removed before the grout is sufficiently strong. Since borehole walls are usually smooth, the bond between grout and borehole wall is the critical strength. The relationship for sufficient strength in a borehole is expressed using Eq. 2.24 (Axelsson, 2009).

$$\tau_f \geq \frac{r_b}{2} \cdot \frac{P_{borehole}}{x} \quad \text{Eq. 2.24}$$

Where the borehole radius is expressed using r_b , acting pressure, $P_{borehole}$, and grouted distance x . The risk of backflow can be reduced by ensuring sufficient penetration length.

When grouting takes place there are two different hydraulic gradients – one for the water and one for the grout. To avoid mechanical breakdown of the grout, it is necessary to carry out the grouting with a gradient in the grout that is larger than the hydraulic gradient (Axelsson, 2009). This is done by ensuring that the initial strength of the grout is sufficient to withstand forces from water. By fulfilling the criteria presented in Eq. 2.25 and Eq. 2.26 it is possible to reduce the risk of mechanical breakdown caused by erosion, fingering or backflow.

$$\tau_{grout} \geq \tau_{water} \quad \text{Eq. 2.25}$$

$$\tau_{grout} \geq \frac{\rho_w \cdot g \cdot b}{2} \cdot \left(-\frac{dh}{dx}\right) \quad \text{Eq. 2.26}$$

Aperture size, b , and hydraulic gradient, $-dh/dx$, are therefore the governing parameters of the rock. Figure 21 shows the shear stress from water as a function of the hydraulic gradient and aperture size.

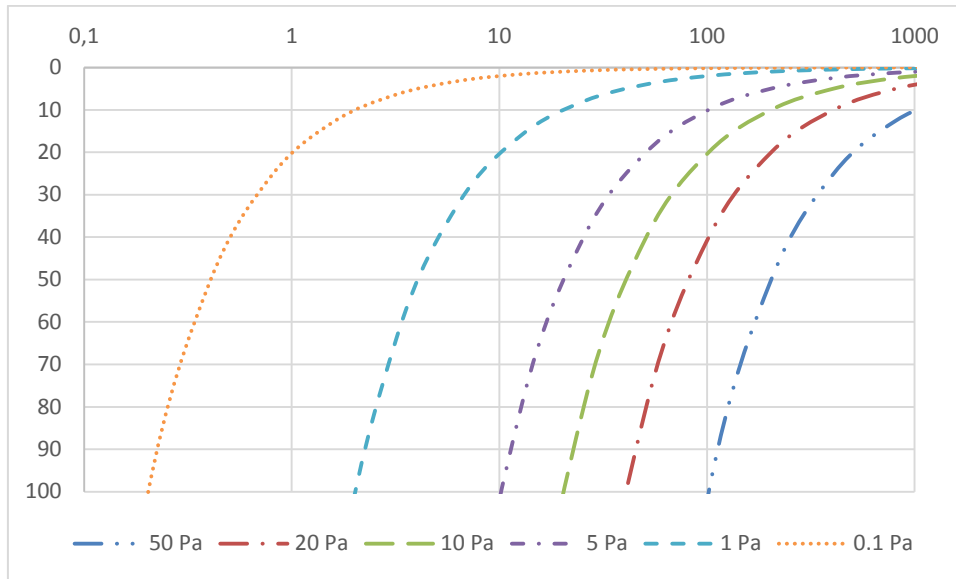


Figure 21. The shear stress from water as a function of the fracture aperture and hydraulic gradient Modified and redrawn from Axelsson (2009).

As for erosion of grouting material in fractures, erosion of fracture filling can also occur due to flowing water in rock. Erosion of the fracture filling can cause redistribution of material and affect the hydrogeological properties of the rock, such as the transmissivity (Axelsson, 2009). The criteria for avoiding erosion of grouting material also apply to erosion of fracture filling material, i.e. the strength of the fracture filling material must be greater than the erosive forces of the water. In general, bond strength between the fracture wall and the existing minerals are magnitudes greater than the erosion forces of flowing water. However, this does not apply to fracture gouge and low-strength weathering products such as clay. The clay is formed from chemical weathering of silicate products. Formation of the clay is dependent on the origin of the silicate minerals, i.e. different clay minerals are formed. As the surrounding confining stress increases, the shear strength of the clay will increase. The strength of the clay will increase with depth. Confining stress in a fracture is generally high but can also be low in the worst cases, resulting in low-strength clay (Axelsson, 2009).

3 Results

The main results of the thesis will be presented in the following chapters. Detailed results for the hydraulic gradient, groundwater shear stress and observation notes can be found in Appendix 1. The chapter will display the results from the inflow and pressure data, the transmissivity and fractures apertures. Penetration length, hydraulic gradient, shear strength of silica sol and the groundwater shear stress will also be published. Finally findings from the visit to the TASS will be displayed.

3.1 Rock mass and fractures interpretation

Firstly, it is likely that the borehole will intersect a couple of fractures that are water-bearing. Total inflow from each borehole is therefore the sum of the inflow from all water-bearing fractures intersected by the borehole. It is also assumed that each fracture is independent and does not interact with other fractures. The flow is assumed to be two-dimensional and the hydraulic properties of the fractures are statistically independent.

3.2 Inflow and pressure analyses

As described in Chapter 1.3.4 two fans were drilled, measured and grouted. A control fan was drilled between each set of fans and was analysed before post-grouting took place. The average natural inflow, maximum inflow and maximum pressure for the tunnel section are presented in Table 1. It should be noted that the maximum inflow and maximum pressure do not necessarily come from the same borehole. The structure in Table 1 is based on the grouting fan layouts, i.e. the control holes are between previously grouted boreholes.

It can be seen that the average inflow from control fans S2C and S2CC in the walls and floor is lower than the inflow measured from the surrounding fans. Inflow from control fan S1C, however, is much higher than the inflow from the surrounding fans, with a maximum inflow from one borehole of 50.4 l/min. Maximum volumes from nearby fans, S1A and S1B, also show high maximum values although they are relatively low compared with S1C. The maximum pressure was also measured in fans S1B and S1C and these results indicate that the fans intersect a large water-bearing fracture.

Control holes located in the roof all show lower average inflow than the surrounding fans, except fan T2CCC. Overall, there is less inflow from the roof than from the floor and walls, and only fans T1A and T2CCC show higher values than other fans in the roof. It can be concluded from these results that a certain degree of sealing has been achieved although the sealing outcome for fans S1A and S1B was not good.

Table 1. Maximum inflow and maximum pressure for the tunnel section. The left-hand side of the table shows the results from the walls and floor and the right-hand side shows the results from the roof.

Fan	Average inflow	Max inflow	Max pressure	Fan	Average inflow	Max inflow	Max pressure
	[l/min]	[l/min]	[MPa]		[l/min]	[l/min]	[MPa]
S1A	0.2	1.7	1.9	T1A	0.04	0.18	0.7
S1C	5.5	50.4	3.5	T1C	0.006	0.023	1
S1B	0.9	9	3.4	T1B	0.005	0.03	1
S2C	0.05	0.52	1.1	T2C	0.005	0.019	0
S2A	0.1	0.47	0.6	T2A	0.008	0.047	0.5
S2CC	0.009	0.06	0.8	T2CC	0.001	0.0047	0
S2B	0.1	1.43	2.6	T2B	0.005	0.04	0.5
				T2CCC	0.023	0.13	2.2

3.3 Fracture transmissivity and apertures

To estimate the transmissivity of fractures, an assumption or simplification needs to be made. The transmissivity calculations are based on natural inflow from the boreholes.

Based on a Pareto distribution, the average transmissivity for the walls and floor of the tunnel section after post-grouting was found to be $T_{av} = 9.9E-08 \text{ m}^2/\text{s}$. This transmissivity is based on all fans in the walls and floor. Control fans reported transmissivity of a similar magnitude to the surrounding fans. The average transmissivity of the roof was found to be $3.5E-08 \text{ m}^2/\text{s}$. All control fans in the roof, except T2CCC, reported no transmissivity since no pressure or inflow were measured.

Aperture calculation is therefore based on the transmissivity obtained from the Pareto distribution. Aperture size results for the tunnel section can be seen in Table 2.

Table 2. Size of apertures based on a Pareto distribution. The left-hand side of the table shows the results for the walls and floor and the right-hand side shows the results for the roof. *Measurements based on one borehole

Fan	Average [μm]	Min [μm]	Max [μm]	Fan	Average [μm]	Min [μm]	Max [μm]
S1A	35	17	93	T1A	32	24	38
S1C	51	15	157	T1C	-	-	-
S1B	44	9	92	T1B*	38	-	-
S2C	24	4	62	T2C	-	-	-
S2A	36	11	61	T2A*	56	-	-
S2CC	21	-	-	T2CC	-	-	-
S2B	24	11	47	T2B*	20	-	-
				T2CCC	20	18	22

3.4 Penetration length based on natural inflow

The maximum penetration length of injected grout in the walls and floor is presented in Figure 22 and for the roof in Figure 23. The penetration length is based on the natural inflow measured from the boreholes, i.e. the transmissivity and aperture are obtained using a Pareto distribution, which can be found in the previous chapter.

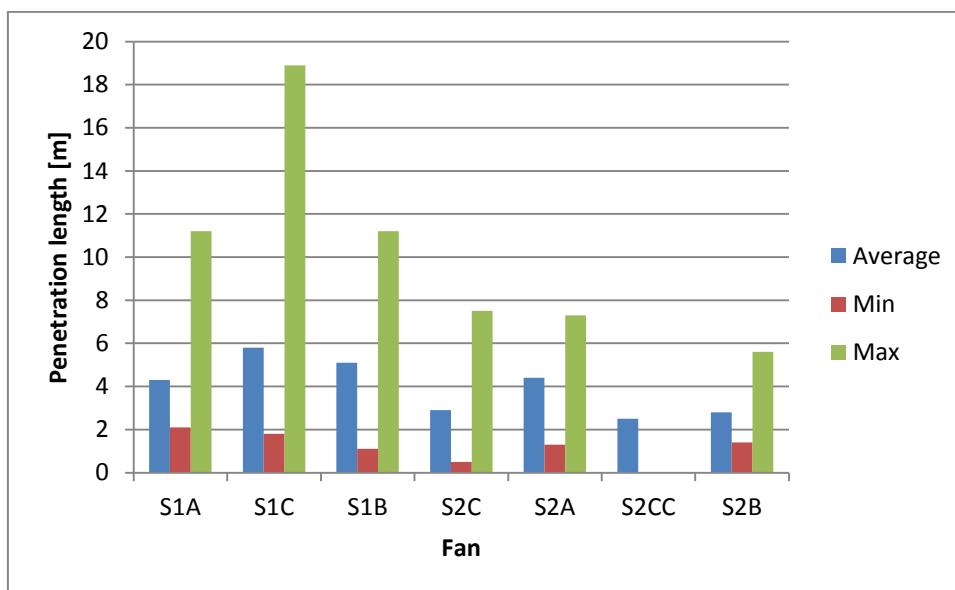


Figure 22. Maximum penetration length of grouting material in the walls and floor. The figure shows the minimum, maximum and average value of the maximum penetration length for each fan.

The maximum values in Figure 22 show the maximum penetration length in the fractures with the largest aperture. These fractures are assumed to transmit 70% of the flow according to the Pareto distribution. To achieve a good sealing outcome, a 50% overlap of grouting material is required. Between (A) and (B) fans, a minimum penetration length of 4.5 m is required and between the control holes (C) and the primary grouted holes (A&B), a minimum penetration length of 2.25 m is required. The distance between boreholes in each fan is approximately 2.5-3 m and to obtain a 50% overlap a penetration length of 1.9-2.25 m is required. All fans meet these requirements for the maximum penetration length.

However, by examining the minimum aperture to achieve a 50% overlap, it can be seen that fractures with an aperture of less than 37 μm will not reach a penetration length of 4.5 m. Fractures with an aperture of less than 19 μm will not reach a penetration length of 2.25 m and fractures with an aperture of less than 17 μm will not reach a penetration length of 1.9 m. These results are based on Eq. 2.18Eq. 2.18 with the following injection settings: Δp 30 bar, gel induction time 720 sec and initial viscosity 0.005 mPas. These settings were used for most of the boreholes during grouting.

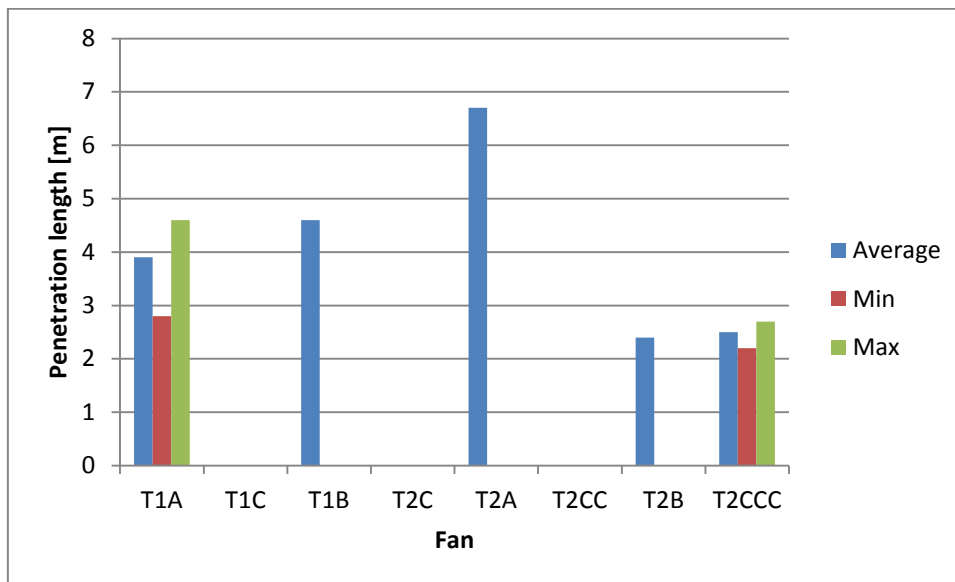


Figure 23. Maximum penetration length of grouting material in the roof. The figure shows the minimum, maximum and average maximum penetration length for each fan.

As can be seen from Figure 21, fans T1C, T2C and T2CC do not show any penetration length since no natural inflow was measured from them. Since little or almost no natural leakage was discovered from the boreholes located in the roof, the penetration length shown in Figure 21 is not accurate.

3.5 Hydraulic gradient

The hydraulic gradient was estimated by four different methods, theoretical, simplified, 'worst case' and according to the geometry. Results are presented in following sub-chapters.

3.5.1 Theoretical gradient

The theoretical hydraulic gradient for three different conditions is presented in Table 4. A description of the parameters used in the calculations can be found in Chapter 2.3.4 and the values used in Table 3. It should be noted that the transmissivity used for the undisturbed rock can show different values over the tunnel stretch, for this case it is assumed that the transmissivity is in the magnitude $T_0 = 1E-07 \text{ m}^2/\text{s}$.

Table 3. Input parameters for calculation of the theoretical gradient and transmissivity.

Tunnel condition	q [l/min/16m]	H [m]	r_t [m]	$\ln(2H/r_t)$ [-]	t [m]	$\ln(1+t/r_t)$ [-]	ξ [-]
After pre grouting	0.8	450	2.25	6	1.5	0.51	5
After post grouting	0.6	450	2.25	6	5	1.17	5
Current	2	450	2.25	6	5	1.17	5

Table 4. Transmissivity and theoretical hydraulic gradient acting over the sealed zone.

Tunnel condition	T_{gr}	dh/dr
After pre grouting	1.53E-10	231
After post grouting	2.62E-10	52
Current	8.95E-10	51

3.5.2 Simplified and 'worst case' gradient

Before grouting is performed, a simplification can be made to estimate the possible hydraulic gradient. In both cases natural inflow and pressure measurements are performed. The simplified hydraulic gradient can be described as follows:

- Pressure is measured at the location of the packer and the distance is therefore from the packer to the borehole opening.

The worst case scenario for estimating the hydraulic gradient can be described as follows.

- It is assumed that the fracture that contributes most flow is located in the same place as the packer and lies perpendicular to the tunnel wall. This will give the shortest distance from the point at which the pressure is measured.

Both cases provide a rough estimation of the hydraulic gradient but can give an indication of high hydraulic gradient before grouting is performed. For the calculations, only boreholes with an inflow higher than 0.1 l/min were considered. In total, 39 boreholes in the walls and floor were considered problematic and nine boreholes in the roof. The average and maximum hydraulic gradient values for the tunnel section can be seen in Table 5.

Table 5. Average and maximum hydraulic gradient for both the simplified and 'worst case' methods.

	Walls and floor [m/m]		Roof [m/m]	
	Average	Max	Average	Max
Simplified method	26	85	15	55
“Worst case” method	51	170	31	110

When the simplified method was used for the walls and floor, fans S1B and S1C showed a higher average hydraulic gradient than the total average, i.e. 41 m/m and 38 m/m respectively. This was also the case in the 'worst case' method, i.e. 82.5 m/m and 77 m/m respectively.

Of the nine boreholes inspected in the roof, three indicated a high hydraulic gradient, which could cause problems – one borehole in fan T1A and two boreholes in fan T2CCC. Both boreholes in fan T2CCC revealed high gradients – 50 m/m and 55 m/m.

The results for all the boreholes, using both the simplified method and the 'worst case' method, can be found in Appendix 1.

3.6 Shear stress of water – Erosion

Knowing the fracture aperture and the hydraulic gradient, an estimation of the shear stress caused by inflow can be made. The average, minimum and maximum values of the shear stress for each case can be seen in Table 7.

Table 7. Shear stress caused by water.

Shear stress of water [Pa]			
	Average	Min	Max
Simplified method	5	0	37
'Worst case' method	10	0	66
According to geometry	13	1	64

As for the hydraulic gradient, high shear stress values can also be found in fans S1B and S1C. The average shear stresses found in fans S1B and S1C, based on the geometry, are 19 Pa and 24.5 Pa respectively. According to the 'worst case' method and geometry, only three boreholes have a shear stress higher than 40 Pa while all the boreholes in the simplified method are below 40 Pa.

3.7 Field trip to TASS

A field trip to the Äspö HRL and an inspection of the TASS Tunnel took place on May 6, 2014. Before the inspection, an analysis of the hydraulic gradient and the shear stress was made. The results from the analysis indicated where leaking boreholes could be found.

Observations were made and boreholes were examined to determine if they were leaking or not. Boreholes were categorised as not visible, tight, moist or leaking. A borehole was considered to be leaking if water was flowing constantly or dripping from it. In total, 24 boreholes were examined in the walls and eight in the roof as well as all the boreholes in floor that were not visible. As construction of the tunnel is complete, the floor has been paved and it was therefore not possible to examine the boreholes in the floor. There were 17 boreholes in the floor that were not visible. Table 8 shows the number of boreholes under different conditions.

Table 8. Visual inspection of leaking boreholes.

	Walls	Roof
Not visible	2	0
Tight	3	3
Moist	10	4
Leaking	9	1

In the roof, three boreholes showed high hydraulic gradients and shear stresses according to the pre-investigation. One was located in fan T1A and two in fan T2CCC. Observations revealed that no boreholes in fan T2CCC leaked and the borehole in T1A was considered moist.

During the inspection, 12 leaking/moist boreholes were discovered. According to the pre-investigation, these boreholes were not expected to leak as they reported a low hydraulic gradient and low shear stresses.

The observations revealed that more boreholes than expected were leaking or were moist.

4 Discussion

The main aim of this report was to develop a hypothesis that describes why leaking boreholes occur even though a tunnel is supposed to be sealed. A good interrelationship between geology, hydrogeology, grouting material properties and grouting procedure will result in successful sealing.

Interpretation of fractured rock mass is a difficult task. Although geological mapping can provide valuable information about the conditions and how the rock is fractured, a large number of assumptions need to be made and to make it possible to describe the rock suitable for the purpose of this thesis. This also applies to the hydrogeological conditions, i.e. how water flow in fractured rock can be described. In this report it was assumed that the flow is two-dimensional and that fractures do not interact, i.e. the hydraulic properties of fractures are independent. This can be true for the surroundings close to the borehole. However, further away from the borehole the fractures are likely to intersect each other and a combination of flow dimensions is possibly a better option to describe the flow.

By comparing control holes and boreholes grouted earlier in the walls and floor, it can be seen that inflow decreases for two of the control fans. However, inflow from control fan S1C is much higher than the surrounding fans. According to the geology, large, water-bearing fractures intersect fans S1B and S1C. Since control fan S1C shows a much higher inflow than nearby fans, it is likely that the fan has hit a fracture plane that did not intersect the same fractures in fans S1A and S1B. Two other interpretations are that part of this fracture could have a larger aperture than the other parts or that the flow is channelled into the fracture plane and the S1C fan hits one of these larger flow paths. One borehole in fan S1C has therefore intersected a more heavily flowing part of the fracture or another fracture plane, contributing to the flow of 50.4 l/min.

The transmissivity of the rock was estimated using a Pareto distribution, where it is assumed that 70% of the borehole inflow originates from one fracture. From the results of the transmissivity it was possible to calculate the aperture size based on the cubic law. For fans located in the walls and floor, the average aperture size was in the range 21-51 μm and with a maximum size of 157 μm , found in fan S1C, which is the controlling fan for fans S1A and S1B. It is assumed in the post-grouting design that silica sol would be suitable for apertures up 150 μm and a cement-based grouting material was thus possibly a better option for fan S1C. The average aperture size for the roof was in the range 20-56 μm with a maximum size of 56 μm . The average aperture for the walls, floor and roof indicates that silica sol was suitable for post-grouting, except for fan S1C. When using a Pareto distribution to describe transmissivity in a borehole, it should be borne in mind that the distribution does not show the physical properties and is an approximation.

Based on the maximum penetration length achieved from maximum transmissivity and corresponding aperture, a successful penetration length with a 50% overlap is achieved in the largest apertures. However, a successful overlap was not achieved for smaller apertures. One of the aims in the fine sealing project was to seal apertures down to 10 μm . It has been shown that silica sol can grout apertures down to 10 μm although the penetration length in such a small aperture also needs to be considered. The maximum penetration length for a 10 μm aperture according to Eq. 2.18 and the design used in the formula is 1.2 m. In Eq. 2.18 the dominant parameters are the pressure difference

between injection pressure and acting groundwater pressure and the gel induction time. By increasing the value of these parameters a longer penetration length can be achieved. Gel induction time is dependent on the gel time and a longer grouting time and a higher volume of silica sol are therefore needed to increase the gel induction time. For most of the boreholes, an injection pressure of 65 bar has been used while the acting groundwater pressure was assumed to be 35 bar, resulting in a pressure difference of 30 bar. It should also be noted that the groundwater pressure is based on observation holes from the pre-investigation (Funehag, Unpublished). Since the tunnel is located at a depth of 450 m below the groundwater surface, the groundwater pressure could be a maximum of 45 bar. This would result in a lower pressure difference and therefore a shorter penetration length. To achieve a longer penetration length, this pressure difference needs to be greater, although it is important to apply a lower grouting pressure than the minimum rock stress in order to avoid possible jacking of the rock. High injection pressure can jack the rock and form new pathways for streaming groundwater. In this case it is possibly better to decrease the distance between primary fans and not drill control fans. The gradient is likely to be higher in the control holes and could therefore increase the risk of erosion. This operation is more likely to achieve a better overlap and thus better sealing. However, decreasing the distance between fans and/or increasing the gel induction time is likely to be more time-consuming and would also increase the cost of the project significantly.

The hydraulic gradient was studied using four different aspects in this report: theoretical, simplified, 'worst case' and geometrical. The theoretical gradient acts after pre-grouting showed a high value caused by the thickness of the sealed zone. Pre-grouting in this section took place inside the tunnel contour, resulting in a thin sealed zone, approximately 1.5 m. The thickness of the pre-grouted zone should be considered when the rock is post-grouted. Most of the post-grouting process will therefore take place in undisturbed rock. The undisturbed rock is likely to include large apertures and also a high gradient at great depth, resulting in high shear stress from the groundwater, increasing the risk of erosion.

To provide a better estimation of the hydraulic gradient, field work could be performed where each of the boreholes is divided into sections (using a double packer or similar) to determine the location of the fractures that intersect the borehole. This measure would provide more detailed inflow and pressure data. Another way to estimate the hydraulic gradient would be to measure the pressure differences between boreholes that intersect the same fracture plane.

When the tunnel was being grouted it was assumed that sufficient shear strength of silica sol would be achieved by injecting grout and removing the packer after 80% of the gel time. This assumption is based on findings published by Axelsson (2009) and is discussed in Chapter 2.4.2. The findings are based on a fall-cone test, which is only able to provide results down to 60 Pa. According to these results, the shear strength of the silica sol would be approximately 50 Pa after 80% of the gel time. By examining the results from the estimation of the shear stress produced by the inflow and comparing them with the estimated shear strength of silica sol, it can be seen that most of the boreholes fulfil the criteria for erosion ($\tau_g > \tau_w$). However, after the visit to the TASS Tunnel, observations were made and it was obvious that something was affecting the shear strength or shear stress as most of the visible boreholes in the wall leaked.

After the grouting process it is likely that groundwater flow will rearrange and affect the surrounding boreholes that intersect the same fracture plane, resulting in higher shear stress in the surrounding boreholes. This rearrangement of groundwater could increase the risk of erosion in boreholes that were not expected to leak. This is likely to be the reason for leaking boreholes in fan T2CCC, where high pressure was measured from two boreholes and no pressure in the rest of the boreholes. However, during observation all the boreholes in the fan were leaking.

As described earlier, the injection time and the shear strength are based on a line extrapolated from fall-cone results. The shear strength of an early-aging silica sol needs to be investigated further to evaluate shear strength development before the lowest value (<60 Pa) is achieved in the fall-cone test.

Other factors are also deemed to affect the early shear strength development of silica sol, such as temperature and dilution. As mentioned in this report, there is a rule of thumb that the gel time is halved if the temperature is doubled. During post-grouting, the mixing of silica sol and the saline solution took place at a tunnel air temperature of 13-14°C while the temperature of the fractured rock was believed to be approximately 8°C. This difference in temperature could therefore lower the gel time of silica sol and result in lower shear strength after 80% of the gel time. This temperature difference should be taken into account when grouting and should be inspected further.

Dilution of silica sol is also a factor that needs to be considered during grouting, especially when grout is injected into boreholes that are drilled with a negative incline. Accumulated water in boreholes is therefore likely to affect the grouting procedure with a decreasing aggregation rate and increasing gel time, resulting in lower shear strength of the silica sol. This is not valid, however, for all negatively inclined boreholes as some boreholes will accumulate more volume than others. This dilution is difficult to prove since accumulated water is evacuated with a vacuum pump as much as possible before injection of grout. However, accumulation of water should be considered between the vacuum step and commencement of injection. It is likely that some boreholes will accumulate water more rapidly than others. The scenario when the grout is injected into the borehole in which water is present needs further examination. How does the grout react when it is mixed with water? Will it become 'slurry' or will it dilute the silica sol perfectly? The volume of grout injected into each borehole also needs to be considered since there will probably be more dilution in boreholes where less grouting material is used. Table 9 shows examples of different gel times for different mixing ratios.

Table 9. Examples of gel time for different mixing ratio at a temperature of 10° (Funehag, 2012).

Weight ratio	Gel time (10°C)
4:1	22,5 min
4.5:1	30 min
5:1	38 min

In the grouting process, the gel time was usually assumed to be 36 min. The time when injection stops and the packer is removed was then 29 min (80% of the gel time) and the shear strength of the silica sol should therefore be approximately 50 Pa. However, if the gel time increases due to dilution and/or temperature and the same stop time is used, a drop in shear strength will be achieved. See Table 10 for the shear strength for different gel times caused by temperature changes. Mixing of silica sol, for example, was performed inside the tunnel at 14°C and it was assumed that the temperature of the

silica sol was the same when injection starts. The grout was then injected into the rock, which was approximately 8°C and it was assumed that it would quickly reach the same temperature as the rock.

Table 10. Development of silica sol shear strength due to different gel time caused by temperature changes.

Temperature [°C]	Gel time [min]	Stop time [min]	% of gel time	Shear strength [Pa]
14.0	36	29	81%	50
12.4	40	29	73%	28
10.9	44	29	66%	15
9.3	48	29	60%	7
7.8	52	29	56%	4

It is known that the shear strength of silica sol after several of hours/day will reach the magnitude of several kPa. The scenario causing the leakage is likely to be insufficient early shear strength of the silica sol. Erosion during grouting, such as fingering and back-flow, therefore needs to be considered.

5 Conclusion and further work

This study has shown that there is no simple explanation for the cause of the leakage and leakage is most likely to be the result of a combination of different factors. The following factors have been considered and are likely to affect sealing performance.

- All control fans show lower inflow values, except the inflow from fans S1C and T2CCC, which is higher than the surrounding fans. However, control holes in the walls and floor show only limited sealing efficiency, while control holes in the roof show better sealing efficiency.
- The average aperture size indicates that silica sol was the correct option in the grouting design. However, grouting with cement-based grout should have been considered in fan S1C.
- A high hydraulic gradient acting towards the tunnel can be expected.
- The penetration length is sufficient for large apertures and overlap has been achieved. Smaller apertures have not achieved sufficient overlap and are limited due to the pressure conditions and the properties of the silica sol. A decrease in the distance between grouting fans and/or increased gel induction time could improve the overlap efficiency.
- Development of early shear strength, below 80% of the gel time, needs further examination.
- The gel time of silica sol is likely to be longer than expected due to temperature and dilution, resulting in lower shear strength of silica sol after 80% of the gel time.
- The manner in which temperature and dilution affect the gel time needs to be examined further.
- Better layout of the boreholes is required, taking into account both the length and spacing between fans and boreholes.
- Pre-grouting inside the tunnel contour is possibly not a good option.

It can be concluded that it is difficult to explain leakage in post-grouted boreholes in tunnels at great depth. This study has shown that a very high hydraulic gradient can be expected in the pre-grouted zone as well as a high gradient outside the pre-grouted zone. The post-grouting mostly took place in un-grouted rock, which is likely to contain relatively large apertures. With a high hydraulic gradient and large apertures, high shear stress caused by groundwater can be expected, thus increasing the risk of erosion. Other factors that are likely to affect the shear strength of the silica sol are the temperature inside the rock and the dilution of the grouting material during grouting. It is likely that the early shear strength of the silica sol was never sufficient to withstand the groundwater shear stress.

6 References

- Andersson, H., 1998. *Chemical rock grouting. An experimental study on polyurethane foams*, Göteborg, Sweden: Chalmers University of Technology.
- Andersson, P., 2009. *Geology of Fennoscandia*. [Online]
Available at:
http://www.nrm.se/english/researchandcollections/researchdivision/laboratoryforisotopegeology/moreaboutisotopegeology/geologyoffennoscandia.291_en.html
[Accessed 15 February 2014].
- Axelsson, M., 2006. *Strength criteria on grouting agents for hard rock, laboratory studies performed on gelling liquid and cementitious grout*, Göteborg, Sweden: Chalmers University of Technology.
- Axelsson, M., 2009. *Prevention of Erosion of Fresh Grout in Hard Rock*. Gothenburg: Chalmers University of Technology.
- Björnström, J., 2005. *Influence of nano-silica and organic admixtures on cement hydration - A mechanistic investigation*, Göteborg, Sweden: University of Göteborg.
- Björnström, J. et al., 2003. Signatures of a drying $\text{SiO}_2(\text{H}_2\text{O})_x$ gel from Raman spectroscopy and quantum chemistry. *Chemical Physics Letters*, Volume 380, pp. 165-172.
- Boussinesq, J., 1868. Mémoire sur l'influence des frottements dans les mouvements réguliers des fluides. (Study of the effect of friction on the laminar flow of fluids.) *Journal de Mathématiques Pures et Appliquées*, II(13), pp. 377-424.
- Broadchem Industrial, 2005. *Products - Colloidal Silica/Silica Sol*. [Online]
Available at: <http://www.broadchemical.com/Products/SilicaSol.htm>
[Accessed 10 March 2014].
- Dalmalm, T., 2004. *Choice of greouting method for jointed hard rock based on sealing time prediction*, Stockholm: Royal Institute of Technology.
- Darcy, H., 1856. *Les Fontaines Publiques de la Ville de Dijon*, Paris: Dalmont.
- Emmelin, A. et al., 2007. *Rock grouting - Current competence and development for the final repository*, Stockholm: Swedish Nuclear Fuel and Waste Management Co (SKB).
- Fransson, Å., 2008. *Grouting design based on characterization of the fractured rock*, Stockholm: Swedish Nuclear Fuel and Waste Management Co (SKB).
- Fransson, Å. & Gustafson, G., 2006. *Efterinjektering: Inläckageprognos och design - förslag till analys. Report 75*, Stockholm: SveBeFo Swedish Rock Engineering Researches.
- Funehag, J., 2007. *Grouting of Fractured Rock with Silica Sol - Grouting design based on penetration length*. Gothenburg: Chalmers University of Technology.
- Funehag, J., 2012. *Guide to Grouting with Silica Sol - for sealing in hard rock (BeFo Report 118)*, Stockholm: Rock Engineering Research Foundation (BeFo).
- Funehag, J. & Axelsson, M., 2003. Hydrogeological characterisation and sealing of narrow fractures in hard rock - A case study. *Materials and Geoenvironment*, 50(1), pp. 121-124.

Funehag, J. & Emmelin, A., 2011. *Injekteringen av TASS-tunneln*, Stockholm: Swedish Nuclear Fuel and Waste Management Co (SKB).

Funehag, J., Unpublished. *Efterinjekteringen av TASS-tunneln - Design, genomförande och resultat från efterinjektering*, Stockholm: Swedish Nuclear Fuel and Waste Management Co (SKB).

Gale, J. & MacLeod, R., 1990. *Le Messurier P 1990: Site Characterization and Validation - Measurement of Flow Rate, Solute Velocities and Aperture in Natural Fractures as a Function of Normal and Near Stress*, Stockholm: SKB.

Geological Survey of Sweden, n.d. *Bedrock Mapping*. [Online]
Available at: http://www.sgu.se/sgu/eng/geol_kartering/berg_kart_e.html
[Accessed 1 March 2014].

Geological Survey of Sweden, n.d. *The Bedrock of Sweden*. [Online]
Available at: http://www.sgu.se/sgu/eng/geologi/svberg_e.html
[Accessed 15 February 2014].

Gustafson, G., 2012. *Hydrogeology for Rock Engineers*. 1st ed. Stockholm: Rock Engineering Research Foundation (BeFo), .

Gustafson, G. & Fransson, Å., 2005. The use of the Pareto distribution for fracture transmissivity assessment. *Hydrogeology Journal*, Volume 14, pp. 15-20.

Gustafson, G. & Stille, H., 1996. Prediction of Groutability from Grout Properties and Hydrogeological Data. *Tunneling and underground space technology*, Volume 11, pp. 325-332.

Hakami, E., 1995. *Aperture Distribution of Rock Fractures*, Stockholm: Royal Institute of Technology.

Hernqvist, L., Kvarnberg, S., Fransson, Å. & Gustafson, G., 2012. A Swedish Grouting Design Concept: Decision Method for Hard Rock Tunneling. *Geotechnical special publication*, Volume I, pp. 816-825.

Hiscock, K. M., 2005. *Hydrogeology - Principles and practice*. Oxford: Blackwell Science Ltd.

Holmboe, M., Wold, S. & Petterson, T., 2011. Effects of the injected grout silica sol on bentonite. *Physics and Chemistry of Earth*, 36(17-18), pp. 1580-1589.

Kutzner, C., 1996. *Grouting of rock and soil*, Rotterdam, Netherlands: A.A. Balkema.

National Research Council (NRC), 1996. *Rock Fractures and Fluid Flow: Contemporary Understanding and Applications*. Washington, D.C.: National Academy of Sciences.

Nonveiller, E., 1989. *Grouting, theory and practice*, Amsterdam, Netherlands: Elsevier Science Publishers B.V..

Nordquist, R., Gustafsson, E. & Thur, P., 2008. *Groundwater flow and hydraulic gradients in fractures and fracture zones at Forsmark and Oscarshamn*, Stockholm: Swedish Nuclear Fuel and Waste Management Co (SKB).

Pusch, R., 1983. *Stability of bentonite gels in crystalline rock-physical aspect*, s.l.: SKBF-KBS.

Sigurdsson, O. & Hardenby, C., 2010. *Äspö Hard Rock Laboratory - The TASS-tunnel - Geological mapping*, Stockholm: Swedish Nuclear Fuel and Waste Management Co (SKB).

Swedish Nuclear Fuel and Waste Management Co, 2012. *Äspö Hard Rock Laboratory - Annual Report 2011*, Stockholm: Swedish Nuclear Fuel and Waste Management Co (SKB).

Warner, P., 2004. *Practical handbook of Grouting*. New Jersey: John Wiley and Sons.

Winberg, A. et al., 2000. *Äspö Hard Rock Laboratory - Final report of the first stage of the tracer retention understanding experiments*. TR-00-07 ed. Stockholm: Swedish Nuclear Fuel and Waste Management Co (SKB).

Zimmerman, R. W. & Bodvarsson, G. S., 1996. Hydraulic Conductivity of Rock Fractures. *Transport in Porous Media*, Volume 23, pp. 1-30.

Appendix 1 Hydraulic Gradient, Shear stresses and Observation

Fan	Borehole Name	Borehole number	Inflow [l/min]	Pressure [bar]	Simplified Gradient	Shear Stress of Water	Worst Case Gradient	Shear Stress of Water	Gradient acc. to geometry	Shear Stress of Water	Theoretical gradient	Shear Stress of Water	Status
S2B	SS0029B01	5	0.014	4	10	2	21	2			51	5	Leaking
	SS0029B03	7	0.02	2	5	1	10	1			51	7	No
	SS0029B04	8	0.022	16	41	3	82	5			51	3	Not visible
	SS0029G04	9	0.012	13	33	2	67	4			51	3	Not visible
	SS0029G03	10	1.43	26	67	15	133	31	74	17	51	12	Not visible
S2CC	SS0031G05	9	0.04	8	20	2	41	1			51	5	Not visible
	SS0031G01	13	0.01	2	5	1	10	1			51	5	Not visible
S2A	SS0036A04	1	0.47	6	15	4	31	8	26	7	51	13	Not visible
	SS0036A02	3	0.064	5	13	2	26	4			51	7	Leaking
	SS0036B02	6	0.00224	3	4	0	8	0			51	3	No
	SS0036B03	7	0.027	3	8	1	15	2			51	6	No
	SS0036G04	9	0.12	1	3	1	5	2	3	1	51	15	Not visible
	SS0036G01	12	0.12	4	10	2	21	4	14	3	51	10	Not visible
S2C	SS0038A03	2	0.52	4	10	3	21	6	11	3	51	16	Leaking
	SS0038A01	4	0.023	11	28	2	56	4			51	4	Leaking
	SS0038B03	7	0.00035	10	13	0	25	0			51	1	Leaking
	SS0038G04	10	0.005	3	8	1	15	1			51	4	Not visible
S1B	SS0042G01	1B	0.00448	11	28	1	55	2	31	1	51	2	Not visible
	SS0042A03	2B	9	34	85	33	170	66	118	46	51	20	Leaking
	SS0042A02	3B	0.29	18	45	7	90	14	63	10	51	8	Leaking
	SS0042A01	4B	0.79	32	80	14	160	28	111	19	51	9	Leaking

	SS0042B01	7B	0.85	2	5	2	10	5			51	23	Not visible
	SS0042G04	10B	0.00322	2	5	0	10	1			51	4	Not visible
S1C	SS0045A04	1C	0.25	8	16	3	32	6	69	13	51	10	Not visible
	SS0045A02	3C	0.056	11	22	2	44	5	95	10	51	5	Leaking
	SS0045A01	4C	1.27	24	48	11	96	22	67	15	51	12	Leaking
	SS0045B01	5C	8.4	35	70	26	140	52	152	57	51	19	Leaking
	SS0045B02	6C	50.4	24	48	37	96	47	83	64	51	39	Leaking
	SS0045B03	7C	0.18	18	36	5	72	9	63	8	51	7	Leaking
	SS0045B04	8C	0.069	10	20	2	40	5	35	4	51	6	Leaking
	SS0045G01	13C	0.045	24	48	4	96	7			51	4	Not visible
S1A	SS0048G07	1A	0.083	8	20	3	40	5	32	4	51	7	Not visible
	SS0048A09	2A	0.012	4	10	1	20	2	14	1	51	4	Leaking
	SS0048A10	3A	0.089	15	38	4	45	8	52	6	51	6	Leaking
	SS0048A11	4A	0.054	19	48	4	95	8	66	6	51	4	Leaking
	SS0048B07	5A	0.044	6	15	2	30	4	13	2	51	6	Leaking
	SS0048B09	7A	0.322	5	13	3	25	6	11	3	51	12	Leaking
	SS0048G12	8A	0.11	6	15	2	30	5	11	2	51	8	Not visible
	SS0048G10	10A	1.72	4	10	5	20	9	11	5	51	23	Not visible

